ELSEVIER

Biophysical Chemistry 85 (2000) 249–271

Biophysical Chemistry

www.elsevier.nl/locate/bpc

Electroporation of curved lipid membranes in ionic strength gradients ☆

Eberhard Neumann*, Sergej Kakorin

Faculty of Chemistry, University of Bielefeld, P.O. Box 100 131, D-33501 Bielefeld, Germany

Received 8 December 1999; accepted 28 December 1999

Abstract

A thermodynamic theory for the membrane electroporation of curved membranes such as those of lipid vesicles and cylindrical membrane tubes has been developed. The theory covers in particular the observation that electric pore formation and shape deformation of vesicles and cells are dependent on the salt concentration of the suspending solvent. It is shown that transmembrane salt gradients can appreciably modify the electrostatic part of Helfrich's spontaneous curvature, elastic bending rigidity and Gaussian curvature modulus of charged membranes. The Gibbs reaction energy of membrane electroporation can be explicitely expressed in terms of salt gradient-dependent contributions of bending, the ionic double layers and electric surface potentials and dielectric polarisation of aqueous pores. In order to cover the various physical contribution to the chemical process of electroporation-resealing, we have introduced a generalised chemophysical potential covering all generalised forces and generalised displacements in terms of a transformed Gibbs energy formalism. Comparison with, and analysis of, the data of electrooptical relaxation kinetic studies show that the Gibbs reaction energy terms can be directly determined from turbidity dichroism (Planck's conservative dichroism). The approach also quantifies the electroporative cross-membrane material exchange such as electrolyte release, electrohaemolysis of red blood cells or uptake of drugs and dyes and finally gene DNA by membrane electroporation.

Keywords: Membrane electroporation; Lipid bilayer; Transmembrane salt gradient; Spontaneous curvature; Membrane elasticity

☆ Dedicated to Professor Gerhard Schwarz on the occasion of his 70th birthday.

* Corresponding author. Tel.: +49-521-106-2053; fax: +49-521-106-2981.
E-mail address: eberhard.neumann@uni-bielefeld.de (E. Neumann).

0301-4622/00/$ - see front matter
PII: S0301-4622(00)00112-5

1. Introduction

Lipid bilayer membranes are traditionally considered as models for biological membranes. Especially lipid vesicles, with their curved membranes, serve as paradigms for the membranes of intracellular organelles or even for cellular plasma membranes. Of course, the unilamellar model character of the lipid bilayer is strictly only applicable to the lipid part of the biomembranes. Ultrastructurally, the cellular plasma membranes are normally embedded in a complex layer structure, where the outer part can be a network of basal structures and special proteins of the inner part of the membrane are connected to various cytoskeletal filament networks.

Because of the high complexity of the shell structure, biomembranes are different compared with the compositionally much simpler lipid bilayers. However, many electromechanical properties are fundamentally the same, qualitatively. Quantitatively, however, it is remarkable that biological membranes scale well with lipid bilayers [1].

There is, however, a particular feature that is characteristic for all living biomembranes and that is often neglected in the study of membrane structure and function. Biomembranes are ubiquitously associated with relatively high electric fields. The natural electric potential difference $\Delta\varphi_{nat}$ across the dielectric (lipid) parts may be as large as $\Delta\varphi_{nat} = \varphi_{in} - \varphi_{out} = -200$ mV, where the outside potential level φ_{out} is set zero as a reference for the inner part $\varphi_{in} < 0$. The natural membrane voltage $U_{nat} = -\Delta\varphi_{nat}$ defines the natural electric field strength $E_{nat} = U_{nat}/d = -\Delta\varphi_{nat}/d$ in a membrane of thickness d; usually we set $d = 5$ nm, covering the dielectric part of the lipid bilayer. Hence $U_{nat} = 200$ mV yields $E_{nat} = 40$ MV m^{-1} (or 400 kV cm^{-1}). In nerve membranes we encounter $U_{nat} = 70$ mV, i.e. $E_{nat} = 14$ MV m^{-1} (or 140 kV cm^{-1}). Compared with technical fields of $U = 220$ V across 2.0-cm pin distance yielding $E = 0.11$ kV cm^{-1}, the biofield strengths are enormously high [2].

Artifical lipid bilayers may be only associated with (natural) electric fields if they contain ionically charged lipids, such that the surface potential difference $\Delta\varphi_s = \varphi_{in} - \varphi_{out}$ may be different from zero. This can be achieved in two different ways: either the number of ionic lipids is different in the two leaflets composing a bilayer or, at equal numbers, the ionic strength on both sides of the membrane is different causing different charge screening thus different values of the surface potential φ_s. A further source for a yet small, but finite value of $\Delta\varphi_s$ may arise when on one side of the membrane there is a high concentration of sucrose (or other material) affecting the dielectric screening constant ε thus changing the coulombic interaction forces.

Indeed, for some time it is known that extent and rate of electric pore formation in lipid vesicles and cells strongly depend on the difference of salt concentration between the interior compartment and the outside solution, as well as on the presence of sucrose or other substances used to control the osmotic balance [3]. It turns out that the theoretical analysis of these observations is very elaborate. Even more demanding is the direct analysis of secondary phenomena of ME such as the electrohaemolysis of red blood cells or the electroporative transfer of dyes and drugs; see below. Analysis so far has been performed on a scaling basis [2,4,5].

Here we conceptionally rationalise these gradient effects and derive quantitative expressions connecting the difference in the salt concentration with the experimental quantities.

2. Thermodynamic theory of membrane electroporation

2.1. Chemical model for the electroporation cycle

As outlined previously, membrane electroporation (ME) can be viewed as a cooperative transition of a cluster L_m of m lipids from a closed state **C** to electroporated states **P** according to [4,5]:

$$\mathbf{C} \underset{k_{-p}}{\overset{k_p}{\rightleftharpoons}} \mathbf{P} \tag{1}$$

These m lipids form the pore edge. Pore formation also involves the entrance of bulk water into

the pore interior, thus leading to hydrophobic and hydrophilic pores.

The degree of ME is given by the fraction f_p of pores:

$$f_p = \frac{[P]}{[P]+[C]} = \frac{K}{1+K} \tag{2}$$

where the equilibrium constant is conventionally defined as:

$$K = \frac{[P]}{[C]} = \frac{f_p}{1-f_p} = \frac{k_p}{k_{-p}} \tag{3}$$

In Eqs. (2) and (3), the concentration brackets refer to a lipid cluster L_m with $m \geq 12$ [6]; k_{p} and $k_{-\mathrm{p}}$ are the rate constants of poration and pore closing, dominant in resealing, respectively.

2.1.1. Relaxation kinetic approach

The time constant of the reaction in Eq. (1) is field-dependent [3]. Chemical relaxation kinetic analysis [7,8] shows that

$$\frac{1}{\tau} = k_p + k_{-p} = k_{-p}(1+K) \tag{4}$$

Typically, at fields $E \approx 5$ MV m^{-1} (50 kV cm^{-1}), we have $\tau \approx 10^{-6}$ s, $K \approx f_p = 10^{-2}$ such that $k_{-\mathrm{p}} \approx 10^6$ s^{-1} and $k_{\mathrm{p}} \approx k_{-\mathrm{p}}K \approx 10^4$ s^{-1}. The field dependence of K and τ gives insight into the molecular mechanism of ME in electric fields; in particular, numerical values of the mean pore radius are obtained. Usually, Eq. (1) has to be extended to cover the more complicated electroporation-resealing kinetics [9,10]. Because the condition $K \ll 1$ always holds, it is the overall cluster rate coefficient $k_{-\mathrm{p}}$ for the closing process, different from previous interpretation [2], that is the dominant field-dependent term in Eq. (4). This suggests that **P** represents at least two pore states: possibly hydrophobic (HO) and hydrophilic (HI), respectively, as explicitly treated previously [11], where $1/\tau \approx k_1/K$ and $K = K_1 \cdot (1+K_2) \approx K_1 \cdot K_2$ were used. Note that τ is the mean open-time of the pore.

2.1.2. Mean pore radius

As a consequence of field-induced water entrance during ME, the membrane surface area S increases by $\Delta S_p = S^P - S_o$ from the zero-field value $S_o = 4\pi a_0^2$, where a_0 is the radius of a spherical lipid vesicle or the nominal mean radius of a cell, up to $S^P = S_0 + \Delta S_p$. The ME data are consistent with the definition of the pore fraction as the relative surface increase [8]:

$$f_p = \frac{\Delta S_p}{S_0} = \frac{N_p \cdot \langle r_p^2 \rangle}{4a_0^2} \tag{5}$$

where N_p is the number of pores of mean pore radius $\bar{r}_p = \langle r_p^2 \rangle^{1/2}$ in a vesicular or cellular membrane (V). Generally, in external electric fields the increase in surface area $\Delta S = \Delta S_p + \Delta S_{ss}$ is composed of two contributions. Besides ΔS_p, the field induced Maxwell stress causes stretching of the membrane (thinning) and the smoothing of undulations. Both ΔS_p and ΔS_{ss} are oftenly separable on the time scale of microseconds [9].

2.2. Transformed Gibbs reaction energy

The experimentally accessible quantity f_p, and thus K, and the energetics of the reaction cycle in Eq. (1) are connected by the fundamental relationship for isobaric (p) isothermal (T) conditions [12].

$$K = \mathrm{e}^{-\Delta_r \hat{G}^{\ominus}/RT} \tag{6}$$

In Eq. (6), $\Delta_r \hat{G}^{\ominus} = \hat{G}_m^P - \hat{G}_m^C$ is the standard transformed Gibbs reaction energy, $R = \mathrm{k}\ N_A$ the general gas constant, k the Boltzmann constant and N_A the Loschmidt–Avogadro constant; T is the absolute (Kelvin) temperature. The quantities $\hat{G}_m^{\alpha}$, where $\alpha = \mathbf{P}$ or $\mathbf{C}$, respectively, are formally the standard values (for 1 M transition) of the transformed chemophysical potentials $\hat{\mu}$. Explicitly, $\hat{G}_m^{\alpha} = (\Sigma_j \nu_j \hat{\mu}_j^{\ominus})_m^{\alpha}$ refers to the (molar cluster of the) m lipids ($j = L$) of the pore edge and to all those solvent molecules ($j = W$) changing from the bulk into the pore interior. Note that here the proper characteristic chemical potentials $\hat{\mu}_j = (\partial \overline{G}/\partial n_j)_{p,T,n \neq n_j}$, where n_j and ν_j are the molar amount and the stoichiometric coefficient of molecule j, respectively, have the quality of *gen-*

eralised chemophysical potentials. The index $n \neq n_j$ means all n constant except for n_j (see Appendix A).

It is recalled that in an applied electric field E, the correct criteria for directional spontaneity (<0) towards equilibrium stationarity ($=0$) of a chemo-electrical process are only met with the transformed Gibbs function [2,12]: $d\hat{G}_{p,T} \leq 0$. The definition of the reaction operator $\Delta_r = d/d\xi$ is given in the context of Eq. (A20).

2.2.1. Reaction energetics of membrane electroporation

Eqs. (2) and (6) provide the basis for the experimental determination of the Gibbs reaction energy terms. Substitution of Eq. (6) into Eq. (2) yields:

$$f_p = \frac{e^{-\Delta_r \hat{G}^{\ominus}/RT}}{1 + e^{-\Delta_r \hat{G}^{\ominus}/RT}} \tag{7}$$

Usually $f_p \ll 1$ (in the order of $\leq 10^{-2}$) and hence the approximation

$$f_p = K = e^{-\Delta_r \hat{G}^{\ominus}/RT} \tag{8}$$

is practically always applicable.

Sometimes it is very appropriate to group together certain energy terms such that we can write Eq. (6) in the form:

$$K = K_0 \cdot e^{X/RT} \tag{9}$$

Where $K_0 = e^{X_0/RT}$. Here, X_0 refers to all terms $\Sigma_k (x_k X_k)_0$ which can be considered *independent* of those variables which are explicitly covered in X, referring to $\Sigma_k x_k X_k$, and not in X_0.

Eq. (9) has been previously used in the form [13,6]:

$$K = K_0 \cdot e^{-\Delta_r \hat{G}_{pol}/RT} \tag{10}$$

where

$$\Delta_r \hat{G}_{pol} = -\int_0^E \Delta_r M \, dE \tag{11}$$

is the transformed electric Gibbs reaction energy. Eq. (10) is suited if it is only the dielectric polarisation term that is field-dependent. K_0 refers to the chemical term

$$\Delta_r G^{\ominus}_{chem} = \Sigma_\alpha \Sigma_j \left(\nu_j \mu_j^{\ominus}\right)^{\alpha}_m = \Sigma_j \left(\nu_j \mu_j^{\ominus}\right)^{P} - \Sigma_j \left(\nu_j \mu_j^{\ominus}\right)^{C} \tag{12}$$

and $\Delta_r M = M_m^P - M_m^C$ is the molar difference in the cluster transition (L_m) from $\alpha = \mathbf{C}$ to $\alpha = \mathbf{P}$. It is recalled that the ordinary chemical potential of species j is defined by

$$\mu_j = \mu_j^{\ominus} + RT \ln a_j$$

where $a_j = c_j y_j / c^{\ominus}$ is the thermodynamic activity (or the absolute value of the effective concentration), c_j the molar concentration and y_j the thermodynamic activity coefficient of species j, respectively; $c^{\ominus} = 1\ \mathrm{mol/dm^3} = 1\ \mathrm{M}$ is the concentration unit. In the expression for the reaction term $\Delta_r G^{\ominus}_{chem} = -RT \cdot \ln(a_m^P / a_m^C)$ covering the cluster of size m, the activity coefficients appear in the ratio $a_m^P / a_m^C = (c_m^P / c_m^C)(y_m^P / y_m^C)$. Since ME hardly will change the y_j coefficients, we safely can set $y_m^P = y_m^C$, thus $a_m^P / a_m^C = c_m^C / c_m^P$. Therefore, the chemical term, against intuition, can be considered as independent on the ionic strength.

2.2.2. Ionic strength dependent reaction terms

The description of salt effects on K, and thus on f_p, requires that X in Eq. (9) takes the form:

$$X = -\left(\Delta_r \hat{G}_{pol} + \Delta_r \hat{G}_{dlay} + \Delta_r \hat{G}_{bend}\right) \tag{13}$$

where besides the dielectric polarisation term, the two ionic–electric double layers of a charged membrane are covered in $\Delta_r \hat{G}_{dlay}$ and the curvature effects are represented in the bending reaction term $\Delta_r \hat{G}_{dlay}$; see Eq. (40).

With Eq. (13), Eq. (9) is specified (and applied below) as:

$$K = K_0 \cdot e^{-(\Delta_r \hat{G}_{pol} + \Delta_r \hat{G}_{dlay} + \Delta_r \hat{G}_{bend})/RT} \tag{14}$$

Here, K_0 involves the reaction terms $\Delta_r G_{line}$ of the line tension or edge energy, $\Delta_r G_{tens}$ of inter-

facial tension in the interface between the lipid head groups and the adjacent medium molecules and the chemical term specified in Eq. (12).

2.2.3. Locality of field effects

An externally applied electric field affects the curved membrane of a vesicle or cell as a whole. On the other hand, electropore formation is generally a sparse local event. The local field inducing the pore structure depends on the angle θ between the site considered and the direction of the external field vector. Therefore the field-dependent ME reaction terms are θ-positional averages: pore fraction f_p, and thus K, connected by Eq. (8), directly reflect $\cos^2\theta$-averages [11] (see below).

For this reason it is appropriate to specify first some of the Gibbs energies in terms of the total membrane of one average vesicle or cell, denoted by $G(V)_i$, referring to N_p pores. The respective Gibbs reaction energies $\Delta_r G_i$, here the physical terms $\Delta_r\hat{G}_{\mathrm{dlay}}$ and $\Delta_r\hat{G}_{\mathrm{bend}}$ are generally expressed (and applied below) as:

$$\Delta_r\hat{G}_i = (G_m^P - G_m^C)_i = \frac{N_A}{N_p}\{G(V)_i^P - G(V)_i^C\} \tag{15}$$

2.2.4. Pore fraction and ionic strength gradient

The data analysis and the conceptional understanding of the experimental phenomena are greatly facilitated, if we refer the various parameters at a finite salt concentration (or ionic strength) difference

$$\Delta c = c^{\mathrm{in}} - c^{\mathrm{out}} \tag{16}$$

to those at $\Delta c = 0$, i.e. to $c^{\mathrm{in}} = c^{\mathrm{out}}$, as a reference.

For a given field strength, Eq. (14) can then be written in the operational form

$$K^{\Delta c} = K^0 \cdot \mathrm{e}^{-(\Delta_r\hat{G}^{\Delta c} - \Delta_r\hat{G}^0)/RT} \tag{17}$$

where the definition $K^0 = K_0 \cdot e^{-\Delta_r\hat{G}^0/RT}$ and the equality $K_0^{\Delta c} = \mathrm{K}_0^0$ *were used*.

Recall, the terms $\Delta_r\hat{G}^{\Delta c}$ and $\Delta_r\hat{G}^0$ both refer to the sum $X = -(\Delta_r\hat{G}_{\mathrm{pol}} + \Delta_r\hat{G}_{\mathrm{dlay}} + \Delta_r\hat{G}_{\mathrm{bend}})$. We now introduce the definition

$$\Delta X = (X^{\Delta c} - X^0) = -\left(\Delta_r\hat{G}^{\Delta c} - \Delta_r\hat{G}^0\right) \tag{18}$$

Substitution into Eq. (8) yields

$$f_p^{\Delta c} = f_p^0 \cdot \mathrm{e}^{\Delta X/RT} \tag{19}$$

representing the *central relationship for the analysis of ionic strength effects* on f_p of ME.

2.3. Electric polarisation of curved membranes

For spherical geometry the electric pore formation occurs dominantly in the pole cap areas. Nevertheless, the actual relaxation kinetic data reflect θ-averages of the electric dipole moments M^θ and the actual membrane field strength E_m^θ [11]. The analysis of ionic strength effects, however, requires that at first the transmembrane potential difference $\Delta\varphi_m$ is considered. Hence

$$\Delta_r\hat{G}_{\mathrm{pol}} = -\left\langle \int_0^{E_m} \Delta_r M^\theta \mathrm{d}E_m^\theta \right\rangle = -b\langle\Delta\varphi_m^2\rangle \tag{20}$$

where, in line with the Maxwell definition ($E = -\nabla\varphi$), $E_m^\theta = -\Delta\varphi_m^\theta/d$ and is given by [14]:

$$b = \frac{N_A\pi\varepsilon_0(\varepsilon_W - \varepsilon_L)\langle r_p^2\rangle}{2d} \tag{21}$$

Further on, $\langle\Delta_r M^\theta\rangle = \langle(M_m^P - M_m^C)^\theta\rangle = \langle\Delta_r P^\theta \cdot V_p\rangle$, where $V_p = \pi\langle r_p^2\rangle d$ is the average (induced) pore volume of the assumed cylindrical pore. At the positional angle θ, the reaction polarisation is given by [13]:

$$\Delta_r P^\theta = N_A(P_m^P - P_m^C)^\theta = N_A \cdot \varepsilon_0(\varepsilon^P - \varepsilon^C)E_m^\theta \tag{22}$$

where ε_0 is the vacuum permittivity, $\varepsilon^P = \varepsilon_W = 80$ (water at 293 K) the dielectric constant of the

pore cluster dominated by the aqueous part (W) of the pore state $\alpha = \mathbf{P}$ and $\varepsilon^C = \varepsilon_L$ is that of the closed lipid state $\alpha = \mathbf{C}$.

2.3.1. Transmembrane potential difference

The average of $\Delta\varphi_m$ in Eq. (20) is defined as

$$\langle \Delta\varphi_m^2 \rangle = \frac{1}{2}\int_0^{\pi} \Delta\varphi_m^2(\theta)\sin\theta d\theta \tag{23}$$

where, for $\Delta\varphi_{nat} = 0$, the local transmembrane potential difference is given by [2,13]:

$$\Delta\varphi_m^{\theta} = \Delta\varphi_{ind}^{\theta} + \Delta\varphi_s \frac{|\cos\theta|}{\cos\theta} \tag{24}$$

For spherical shells of radius $a \gg d$, the stationary value of the interfacially (Maxwell–Wagner) induced potential difference $\Delta\varphi_{ind}$ is defined as

$$\Delta\varphi_{ind}^{\theta} = -\frac{3}{2} Ea \cdot f_{\lambda} |\cos\theta| \tag{25}$$

where the conductivity factor f_{λ} can be generally expressed in terms of a and d and the conductivities λ_m, λ_0, λ_i of the membrane, the vesicle (cell) interior and the external solution, respectively. If, as usual, $d \ll a$, $\lambda_m \ll \lambda_0$, λ_i, it can be readily shown that $f_{\lambda} = [1 + \lambda_m(2 + \lambda_i/\lambda_0)/(2\lambda_i d/a)]^{-1}$; for negligibly small membrane conductivity, $\lambda_m = 0$, we have $f_{\lambda} = 1$ [2,14,15]. Indeed, deviations of the respective data from the extrapolation line, obtained from the low-field strength data where $f_{\lambda} = 1$ applies, have been used to determine the finite membrane conductivity due to ME at higher field strengths [6]. Substitution of Eq. (25) into Eq. (24) and then into Eq. (23) yields

$$\Delta_r \hat{G}_{pol} = -\frac{b}{3}\left\{\left(\frac{3}{2} Ea f_{\lambda}\right)^2 + \Delta\varphi_s^2\right\} \tag{26}$$

where $\langle|\cos\theta|^2\rangle = 1/3$ and $\langle|\cos\theta|^2/\cos\theta\rangle = 0$ for the integration boundaries $\theta = \pi$ and $\theta = 0$ was applied. Note that, here too, consistent with Maxwell's definition of the electric field ($E = -\nabla\varphi$) as the negative gradient of the electric potential, $\Delta\varphi_s$ refers to the potential drop for the electrodiffusion of positive ions in the direction of the external field strength vector. In our experimental examples, we may readily neglect the contributions of surface conductance and space charges on the induced potential difference $\Delta\varphi_{ind}$, [15] (see below).

2.3.2. Electrostatic surface potential

As long as the approximation $f_{\lambda}(\lambda_m, \lambda_0, \lambda_i) = 1$ applies, i.e. at very small extents of ME, it is the transmembrane surface potential difference $\Delta\varphi_s$ which is dominant in the ionic strength (I) dependence of the electrostatic surface of interfacial potential φ_s of a (ionic) charged membrane. Adjusted to the directionality specified in Eq. (16) we define here

$$\Delta\varphi_s = \varphi_{in} - \varphi_{out} \tag{27}$$

The Gouy–Chapman theory provides an expression for the I-dependence of φ_s, where the charge screening by the layer of counterions reduces the nominal surface potential φ_S^0 to the actual value φ_s which is equivalent to the reduction of the nominal surface charge density $\sigma_0 = q_0/S$ to a value $\sigma = q_s/S$, where q_0 and q_s are the respective charges and S the surface area.

The solution of the Poisson–Boltzmann equation for the potential φ_s of $z_s/z_i = 1{:}1$ surface charge—free charge interactions yields $\varphi_s(0)$. For the condition of small surface potentials $\varphi_s(x) \ll RT/F \approx 25$ mV, $\varphi_s(x)$ drops with the distance x from the surface (at $x = 0$) according to [16]:

$$\varphi_s(x) = \varphi_s(0) \cdot e^{-x/\ell} \tag{28}$$

where the Debye length (ℓ) is given by

$$\ell = \frac{1}{F}\left(\frac{\varepsilon_0 \varepsilon RT}{2I}\right)^{1/2} \tag{29}$$

and the molar ionic strength is defined by

$$I = \frac{1}{2}\sum_i z_i^2 c_i \tag{30}$$

where z_i is the charge number and c_i the molar concentration (mol/dm^3) of the ion of type i. For

a 1:1 electrolyte, $I = c$, the salt concentration of the electrolyte. Classical plate condensor theory shows that $\sigma = \varepsilon_0\varepsilon_w E = -\sigma\varepsilon_0\varepsilon_w \, \mathrm{d}\varphi_s(x)/\mathrm{d}x$ and $\sigma = \varepsilon_0\varepsilon_w\varphi_s(0)/\ell$. We thus obtain:

$$\varphi_s(0) = \frac{\sigma_s \cdot \ell}{\varepsilon_0\varepsilon_w} \tag{31}$$

Substitution in Eq. (28) for $\sigma_{\mathrm{in}}\ell_{\mathrm{in}}$ and $\sigma_{\mathrm{out}}\ell_{\mathrm{out}}$, respectively, yields

$$\Delta\varphi_s = \frac{1}{F}\left(\frac{RT}{2\varepsilon_0\varepsilon_w}\right)^{1/2}\left\{\frac{\sigma_{\mathrm{in}}}{I_{\mathrm{in}}^{1/2}} - \frac{\sigma_{\mathrm{out}}}{I_{\mathrm{out}}^{1/2}}\right\} \tag{32}$$

Eq. (32) enters into the expression for $\Delta\varphi_m$; see Eq. (24). We now can specify Eq. (26) for the description of the dependence on I_{in} and I_{out}, respectively, according to:

$$\Delta_r\hat{G}_{\mathrm{pol}} = -\frac{b}{3}\left\{\left(\frac{3}{2}Ea f_\lambda\right)^2 + \frac{RT}{2F^2\varepsilon_0\varepsilon_w}\left(\frac{\sigma_{\mathrm{in}}}{I_{\mathrm{in}}^{1/2}} - \frac{\sigma_{\mathrm{out}}}{I_{\mathrm{out}}^{1/2}}\right)\right\} \tag{33}$$

When the salt concentration of the outside solution is very different from that of the inside medium (as it is usually adjusted for efficient ME), the salt gradient appreciably contributes to $\Delta\varphi_m$. In this case, the field effect is enhanced on one pole cap of a vesicle (or cell) and reduced on the other one; see Neumann et al. [2].

2.3.3. Double layer capacitance

Since ME increases the surface of the membrane, the surface charge density decreases and thus also the interfacial potential. Charge conservation for the two states **P** and **C** dictates that $q_s^P = q_s^C = q_s$. Since $q_s = S_0 \cdot \sigma = S^P \cdot \sigma^P$ and using Eq. (5) we see that

$$S^P = S_0(1 + f_p) \quad \text{and} \quad \sigma^P = \sigma(1 + f_p)^{-1} \tag{34}$$

Applying now Eq. (A5) of Appendix A to the ionic double layer condensor of a charged membrane surface with fixed ionic charges, we see that

$$\mathrm{d}G_{\mathrm{dlay}} = \Delta\varphi_{\mathrm{dlay}} \cdot \mathrm{d}q_s = \Delta\varphi_{\mathrm{dlay}} \cdot S\mathrm{d}\sigma \tag{35}$$

where the condensor voltage $U_{\mathrm{dlay}} = -\Delta\varphi_{\mathrm{dlay}}$ refers to the potential difference

$$\Delta\varphi_{\mathrm{dlay}} = \varphi_s(0) - \varphi(\ell) = \frac{\sigma\ell}{\varepsilon_0\varepsilon_w} \tag{36}$$

of the equivalent-condensor with the reference potential $\varphi(\ell) = 0$ and where Eq. (31) was applied. Straightforward electrostatics defines the energy of the condensor as

$$G_{\mathrm{dlay}} = \frac{1}{2}C_{\mathrm{dlay}} \cdot \Delta\varphi_{\mathrm{dlay}}^2 = \frac{\sigma^2 S\ell}{2\varepsilon_0\varepsilon_w} \tag{37}$$

and the capacitance as

$$C_{\mathrm{dlay}} = \varepsilon_0 \cdot \varepsilon_w \cdot S/\ell \tag{38}$$

We now apply Eq. (37) to the electroporative state transition $\mathbf{C} \rightleftharpoons \mathbf{P}$. Insertion of the expressions (34) into Eq. (37) and using the approximation $1/(1 + f_p) - 1 = -f_p/(1 + f_p) = -f_p$ for $f_p \ll 1$ yields the difference term:

$$G_{\mathrm{dlay}}^P - G_{\mathrm{dlay}}^C = -f_p\frac{S_0\sigma^2\ell}{2\varepsilon_0\varepsilon_w} \tag{39}$$

Of course, ME affects both the inside (in) and the outside (out) of the membrane. Using Eq. (5) in the form $f_p S_0 = N_p\pi\langle r_p^2\rangle$ and substitution in Eq. (39) leads to:

$$G(V)_{\mathrm{dlay}}^P - G(V)_{\mathrm{dlay}}^C = -\frac{N_p\pi \cdot \langle r_p^2\rangle}{2\varepsilon_0\varepsilon_w} \times \left\{\sigma_{\mathrm{in}}^2\ell_{\mathrm{in}} + \sigma_{\mathrm{out}}^2\ell_{\mathrm{out}}\right\}$$

Substitution in Eq. (15) for $i = \mathrm{dlay}$ finally yields:

$$\Delta_r\hat{G}_{\mathrm{dlay}} = -\frac{N_A\pi \cdot \langle r_p^2\rangle}{2\varepsilon_0\varepsilon_w}\left\{\sigma_{\mathrm{in}}^2\ell_{\mathrm{in}} + \sigma_{\mathrm{out}}^2\ell_{\mathrm{out}}\right\} \tag{40}$$

2.4. Membrane elasticity parameters

2.4.1. The Helfrich equation

In 1973, Wolfgang Helfrich has proposed an approximation for the surface energy density g_{bend} of bending a bilayer membrane [17]. The widely celebrated Helfrich equation:

$$g_{\mathrm{bend}} = \frac{\kappa}{2}C^2 + \bar{\kappa}C_1C_2 \tag{41}$$

specifies the bending energy modulus κ, a general curvature term

$$C = C_1 + C_2 - C_0 \tag{42}$$

and the elastic modulus $\bar{\kappa}$ of the Gauss curvature C_1C_2, where C_1 and C_2 are the principal curvatures, see Eq. (A10). The parameter C_0 is introduced by Helfrich as the spontaneous curvature. A bilayer membrane may be spontaneously curved if the lipid composition of one monolayer leaflet is different from that of the other leaflet; for instance, the lipid headgroups in one leaflet may be larger than (the hydrocarbon chain thickness) those in the other leaflet. The equilibrium state then is characterised by $C_1 + C_2 = C_0$ with energy contents of $G_0 = \oint g_0 \mathrm{d}S = \bar{\kappa}\oint C_1C_2\mathrm{d}S = \bar{\kappa}\oint(C_0^2/4)\mathrm{d}S$ if $C_1 = C_2$.

The Gauss term $\bar{\kappa}C_1C_2$ remains constant when the topology of an object does not change [18]. In Eq. (41), the obvious reference $g_{\mathrm{bend}} = 0$ refers to the planar membrane with $C_1 = C_2 = C_0 = 0$, of homogeneous composition and equal solution on both membrane sides. Obviously, in classical Gibbs notation, $G_{\mathrm{bend}} = \oint g_{\mathrm{bend}}\,\mathrm{d}S$ holds.

2.4.2. The curvature reaction term

The general bending parameters in the Gibbs equation as suggested in Eq. (A9) of the Appendix A are readily expressed with the Helfrich terms. For $k = 1$, we set $\beta_i = \beta$ and $C_k = C_1 + C_2$; for $k = 2$, we have $C_k = \mathrm{C}_1 \cdot C_2$ and $\beta_i = \bar{\beta}$. Substitution in Eq. (A8) yields

$$\mathrm{d}G_{\mathrm{bend}} = \beta\mathrm{d}C + \bar{\beta}\mathrm{d}(C_1C_2) \tag{43}$$

with the differential terms

$$\mathrm{d}\beta = \kappa C\,\mathrm{d}S \quad \text{and} \quad \mathrm{d}\bar{\beta} = \bar{\kappa}\mathrm{d}S \tag{44}$$

Integration within the respective boundaries yields

$$\beta = \kappa\oint C\mathrm{d}S \quad \text{and} \quad \bar{\beta} = \bar{\kappa}\oint\mathrm{d}S \tag{45}$$

If C is independent of S, the expression $\beta = [\kappa \cdot \oint\mathrm{d}S]\cdot C$ represents Hooke's law, as linear approximation, where terms like C^2 and higher powers are neglected in the series expansion. Substitution of Eq. (45) in Eq. (43) yields

$$\mathrm{d}G_{\mathrm{bend}} = \oint\mathrm{d}S[\kappa C\mathrm{d}C + \bar{\kappa}\mathrm{d}(C_1C_2)] \tag{46}$$

Applied to spherical membranes such as those of lipid vesicles of radius a, we see that $\oint\mathrm{d}S = S = 4\pi a^2$, $C_1 + C_2 = 2/a$ and $C_1C_2 = 1/a^2$. Substitution in Eq. (46) and using Eq. (42) yields:

$$\mathrm{d}G(V)_{\mathrm{bend}} = S\left[\kappa\left(\frac{2}{a} - C_0\right)\mathrm{d}\left(\frac{2}{a} - C_0\right) + \bar{\kappa}\mathrm{d}\left(\frac{1}{a^2}\right)\right] \tag{47}$$

If $S = \oint\mathrm{d}S$ can be considered as practically constant, integration yields

$$G(V)_{\mathrm{bend}} = S\left[\frac{\kappa}{2}\left(\frac{2}{a} - C_0\right)^2 + \frac{\bar{\kappa}}{a^2}\right] \tag{48}$$

using the homogeneous planar membrane boundaries $a \to \infty$ and $C_0 = 0$ for the reference $G(V)_{\mathrm{bend}} = 0$. Note, Eq. (48) refers to a spherical shell. Eq. (48) is now applied to states $\alpha = \mathbf{P}$ and $\alpha = \mathbf{C}$, respectively. Using the approximations $S^P = S_0(1 + f_p) = S_0 = 4\pi a_0^2$ and $a = a_0$ as well as $\kappa^P = \kappa$ and $\bar{\kappa}^P = \bar{\kappa}$, we obtain the difference

$$G(V)^P_{\mathrm{bend}} - G(V)^C_{\mathrm{bend}} = \frac{S_0\cdot\kappa}{2} \times\left[(\mathrm{C}_0^P)^2 - C_0^2 - \frac{4(C_0^P - C)}{a_0}\right] \tag{49}$$

Insertion into Eq. (15) and applying Eq. (5) in the form $S_0/N_p = \pi\langle r_p^2\rangle/f_p$, yields the final curvature reaction term:

$$\Delta_r\hat{G}_{\text{bend}} = B\cdot\left[(C_0^P)^2 - C_0^2 - \frac{4(C_0^P - C_0)}{a_0}\right] \quad (50)$$

where $B = \dfrac{N_A\cdot\kappa\cdot\pi\langle r_p^2\rangle}{2f_p}$.

2.5. Electrostatics of membrane elasticity

Shape and shape deformations of lipid vesicles (and cells) in electric fields have been traditionally described in terms of C_0, κ and $\bar{\kappa}$ [19–22]. Each of these elasticity parameters has been split into a mechanical and an electrostatic part:

$$C_0 = C_0^{\text{el}} + C_0^{\text{mech}}, \quad \kappa = \kappa^{\text{el}} + \kappa^{\text{mech}},$$
$$\bar{\kappa} = \bar{\kappa}^{\text{el}} + \bar{\kappa}^{\text{mech}} \quad (51)$$

At equal chemical composition of the two leaflets of the bilayer membrane and at equal packing density in the two monolayers there is no mechanical contribution to C_0: $C_0^{\text{mech}} = 0$ and $C_0 = C_0^{\text{el}}$. For this case $\Delta_r\hat{G}_{\text{bend}} = \Delta_r\hat{G}_{\text{bend}}^{\text{el}}$. Specifically, Eq. (50) takes the form:

$$\Delta_r\hat{G}_{\text{bend}}^{\text{el}} = B\left\{\left[(C_0^{\text{el}})^P - C_0^{\text{el}}\right] \times\left[(C_0^{\text{el}})^P - C_0^{\text{el}} - 4/a_0\right]\right\} \quad (52)$$

where

$$B = \frac{N_A\pi\langle r_p^2\rangle\kappa}{2\cdot f_p} \quad (53)$$

If electrostatic contributions are dominant, we use the approximations $\kappa = \kappa^{\text{el}}$ and $\bar{\kappa} = \bar{\kappa}^{\text{el}}$. Obviously, ME is enhanced by electrostatic curvature effects if $\Delta_r\hat{G}_{\text{bend}}^{\text{el}} < 0$ holds. This is the case for $C_0 > 2/\bar{a}$, because the surface charge density of the aqueous pore is smaller than that of the equivalent closed state: $(C_0^{\text{el}})^P < C_0^{\text{el}}$.

2.5.1. Cylindrical and spherical shells

The electrostatic contributions to C_0, κ and $\bar{\kappa}$ have been quantified by using the Poisson–Boltzmann equation [16] and the Debye–Hückel approximation for diluted electrolyte solution adjacent to the membrane surfaces [23]. This approach has been used first for monolayers [24], then for symmetric bilayers [25] and for undulating membranes [26]. The theoretical results have proven useful to describe the experimental data [20,27]. Helfrich's concept of spontaneous curvature was found to be especially powerful for the description of bump formation in red blood cells [19] and for membrane inclusions [28].

The C_0 model is equivalent to the area-difference-energy (ADE) model with a renormalised area difference [29,30]. The ADE model has been successfully applied to curvature effects of ME [31]. The parameters C_0^{el}, κ^{el} and $\bar{\kappa}^{\text{el}}$ are readily accessible to experimental determination if the electrolyte concentration on *one* side of a planar or curved membrane can be varied. The theoretical approaches to the curvature parameters have been at first addressed to symmetrically curved membrane shells such as those of a cylindrical membrane tube (cyl) and a spherical vesicle (sph) [24]. A spherical membrane shell is characterised by a mean radius $\bar{a}$ and a thickness d, respectively:

$$\bar{a} = \frac{a_{\text{out}} + a_{\text{in}}}{2}, \quad d = a_{\text{out}} - a_{\text{in}} \quad (54)$$

Applying the celebrated Helfrich equation in the form of Eqs. (41) and (42) to cylinder and sphere geometry, the electrostatic contributions are given by:

$$g_{\text{bend}}^{\text{el}}(\text{cyl}) = \frac{\kappa^{\text{el}}}{2}(C_0^{\text{el}})^2 - (\kappa^{\text{el}}C_0^{\text{el}})\frac{1}{\bar{a}} + \left(\frac{\kappa^{\text{el}}}{2}\right)\frac{1}{\bar{a}^2} \quad (55)$$

$$g_{\text{bend}}^{\text{el}}(\text{sph}) = \frac{\kappa^{\text{el}}}{2}(C_0^{\text{el}})^2 - (4\kappa^{\text{el}}C_0^{\text{el}})\frac{1}{\bar{a}} + (2\kappa^{\text{el}} + \bar{\kappa}^{\text{el}})\frac{1}{\bar{a}^2} \quad (56)$$

Note that for cylindrical shells $\bar{\kappa}(\mathrm{cyl}) = 0$ and the previously used vesicle radius is $a_0 = \bar{a}$.

2.5.2. Elasticity parameters and Debye length

As outlined in Appendix B, theory provides specific expressions with the same expansion characters as those in Eqs. (55) and (56); see Eq. (A22).

For both cylindrical and spherical shells we find that:

$$C_0^{\mathrm{el}} = \frac{2\ell n[(1+\beta_{\mathrm{out}})(1+\beta_{\mathrm{in}})]}{\bar{a}(\gamma_{\mathrm{out}}+\gamma_{\mathrm{in}})} \tag{57}$$

where $\beta = \left(1+\frac{s^2}{4}\right)^{1/2}$,

$$\gamma = \frac{\ell}{\bar{a}}\left(1-\frac{8(1-1/\beta)}{s}\right),$$

$$s = \frac{e_0\sigma\ell}{\varepsilon_0\varepsilon_w kT},$$

and

$$\kappa^{\mathrm{el}} = 2\bar{a}\varepsilon_0\varepsilon_w\left(\frac{kT}{e_0}\right)^2(\gamma_{\mathrm{out}}+\gamma_{\mathrm{in}}) \tag{58}$$

The expression for $\bar{\kappa}^{\mathrm{el}}(\mathrm{sph})$ is quite involved and is given in Appendix B.

For the case of thin shells ($d \ll \bar{a}$) and very low effective, i.e. screened, surface charge densities (at $c \geq 0.1$ M), the parameters are very small: i.e $s = \sigma e_0 \cdot \ell/(\varepsilon_0\varepsilon_w kT) \ll 1$.

In this case ($d \ll \bar{a}$; $s \ll 1$) we obtain:

$$C_0^{\mathrm{el}} = -\frac{2(s_{\mathrm{in}}^2 - s_{\mathrm{out}}^2)}{3\left(s_{\mathrm{in}}^2\ell_{\mathrm{in}} + s_{\mathrm{out}}^2\ell_{\mathrm{out}}\right)} \tag{59}$$

$$\kappa^{\mathrm{el}} = \frac{3}{8}\left(\frac{kT}{e_o}\right)^2\varepsilon_0\varepsilon_w\left(s_{\mathrm{in}}^2\ell_{\mathrm{in}} + s_{\mathrm{out}}^2\ell_{\mathrm{out}}\right) \tag{60}$$

$$\bar{\kappa}^{\mathrm{el}} = -\frac{kT}{4e_0}\left(\sigma_{\mathrm{in}}s_{\mathrm{in}}\ell_{\mathrm{in}}^2 + \sigma_{\mathrm{out}}s_{\mathrm{out}}\ell_{\mathrm{out}}^2\right) \tag{61}$$

Eqs. (59)–(61) explicitly cover the dependencies on the salt concentration via the Debye length and the surface charge densities. If $c^{\mathrm{in}} = c^{\mathrm{out}}$, then the Debye lengths are also equal: $\ell_{\mathrm{in}} = \ell_{\mathrm{out}} = \ell$, and Eqs. (59)–(61) lead to the simple approximations already derived by Winterhalter and Helfrich [23]:

$$C_0^{\mathrm{el}} = -\frac{4d}{3\bar{a}\ell}, \quad \kappa^{\mathrm{el}} = \frac{3\sigma^2\ell^3}{4\varepsilon_0\varepsilon_w}, \quad \text{and}$$

$$\bar{\kappa}^{\mathrm{el}} = -\frac{\sigma^2\cdot\ell^3}{2\varepsilon_0\varepsilon_w} \tag{62}$$

Note, difference from Winterhalter and Helfrich [23], here $2\delta = 2d/\bar{a}$ refers to the difference between $\sigma_{\mathrm{in}} = \sigma(1+\delta)$ and $\sigma_{\mathrm{out}} = \sigma(1-\delta)$, where σ is the charge density of the planar monolayer (equal for the inner and the outer leaflet). For the symmetrically charged curved bilayer $C_0^{\mathrm{el}} < 0$, rationalised by the larger repulsive forces between the charged groups of the inner leaflet, i.e. larger curvature ($1/a_{\mathrm{in}} > 1/a_{\mathrm{out}}$). For a planar bilayer, if the concentration of ions is equal on the two membrane sides, $C_0^{\mathrm{el}} = 0$.

2.5.3. Area difference elasticity

The chemical composition of both the membrane and the adjacent solutions may affect the spontaneous curvature C_0. Different repulsive forces, due to different screening for instance, cause different packing densities. This produces an area difference elasticity (ADE) Gibbs energy [29,30], affecting also ME [31].

At constant area of the midsurface, whose curvature is $C_1 + C_2 = 2/\bar{a}$, the effective area difference (ΔS_0) is given by [30]:

$$\Delta S_0 = \Delta\hat{S}_0 + 2C_0\mathrm{d}\bar{a}^2/\alpha \tag{63}$$

where α is the dimensionless material parameter; for 1-stearoyl-2-oleoyl-*sn*-glycero-3-phosphatidylcholine (SOPC) $\alpha \approx 1$ [20]. The parameter $\Delta\hat{S}_0$ is the relaxed area difference: $\Delta\hat{S}_0 = (N^{\mathrm{out}} - N^{\mathrm{in}})/\phi_0$, where N^{out} and N^{in} are the total number of lipid molecules in the outer and inner leaflets, respectively, ϕ_0 is the equilibrium surface density of the molecules in a monolayer of a flat membrane.

The decrease in the ADE–Gibbs energy due to the formation of N_p cylindrical pores is given by [31]

$$G(V)^P_{\mathrm{ADE}} - G(V)^C_{\mathrm{ADE}} = \frac{\pi\alpha\kappa}{d^2 S_0}\left\{(\Delta S - \Delta S_0^P)^2 - (\Delta S - \Delta S_0)^2\right\} \quad (64)$$

where, $\Delta S\ (\mathrm{sph}) = 2S_0 \cdot d/\bar{a}$ is the total area difference between the neutral surfaces of the two monolayer leaflets and $S_0 = 4\pi a_0$. If $N^{\mathrm{out}} = N^{\mathrm{in}}$ can be used, in particular for large a_0, Eq. (63) yields here $\Delta S_0 = 2C_0^{\mathrm{el}} d\bar{a}^2/\alpha$ and for the pore state we have $\Delta S_0^P = 2(C_0^{\mathrm{el}})^P d\bar{a}^2/\alpha$ using $\bar{a}^P = \bar{a}$. As argued before, $(C_0^{\mathrm{el}})^P < C_0^{\mathrm{el}}$ because of smaller repulsive forces at the inequality $\sigma^P < \sigma$. Again, analogous to Eqs. (49) and (52) we have:

$$\Delta_r \hat{G}^{\mathrm{el}}_{\mathrm{bend}} = \Delta_r \hat{G}^{\mathrm{el}}_{\mathrm{ADE}} = \frac{N_A}{N_p} \times (G(V)^P_{\mathrm{ADE}} - G(V)^C_{\mathrm{ADE}}) \quad (65)$$

If $C_0^{\mathrm{el}} > 2\pi\alpha/\bar{a}$, i.e. $\Delta S_0 > \Delta S$ holds and ΔS_0^P lies in the interval $(\Delta S - [\Delta S - \Delta S_0]) < \Delta S_0^P < \Delta S_0$, we see that $\Delta_r \hat{G}^{\mathrm{el}}_{\mathrm{ADE}} < 0$; hence ME is facilitated. On the other hand, if $C_0^{\mathrm{el}} < 2\pi\alpha/\bar{a}$ or $(\Delta S - [\Delta S - \Delta S_0]) > \Delta S_0^P$ holds, ME leads to an increase in $G(V)_{\mathrm{ADE}}$, thus ME is hindered by the C_0^{el} effect.

2.5.4. Shape deformations

As already mentioned, electrooptical relaxation experiments of lipid vesicles clearly indicate two kinetic phases of membrane surface increase $\Delta S = \Delta S_p + \Delta S_{ss}$ in an external electric field E [9]. The rapid phase ($\tau \approx 0.1$ μs) is consistent with field-induced membrane stretching and smoothing of undulations (ΔS_{ss}) and the slower phase ($\tau \approx 1$ μs) reflects (ΔS_p) of electric pore formation by ME. The relaxation amplitude of the ME-phase reflects the balance between electrical and elastic stresses on the membrane and is characterised by a stationary value $\Delta a_{\max} = \zeta_0$ of the increase in the vesicle radius. Theory provides [22]:

$$\zeta_0 = \frac{\varepsilon_0 \varepsilon_W E^2 \bar{a}^4}{32\kappa(1 - C_0\bar{a}/6)} \quad (66)$$

where the radius occurs in the 4th power rendering $\Delta a_{\max}$ strongly dependent on $\bar{a}$. If $C_0 = C_0^{\mathrm{el}}$ and $\kappa = \kappa^{\mathrm{el}}$ applies, ζ_0 can be strongly dependent on transmembrane salt gradients; see Eqs. (59) and (60). In summary, not only electric pore formation but also the elongation of vesicles and cells and the modulations of these field effects can be rigorously described in terms of our chemophysical model for the electroporation–resealing cycle.

2.5.5. Turbidity dichroism and pore fraction

One of the most powerful techniques to experimentally determine the pore fraction f_p is chemical relaxation spectrometry in electric fields [2,8,13]. Recent progress in instrumentation provides very reliable tools [32] to determine rapid absorbance and turbidity changes in polarised light simultaneously at different light polarisation modes.

In particular, the turbidity modes $\Delta T^-/T_0$ of deformational–orientational dichroism ΔT^-, relative to the turbidity value T_0 at zero field, and the relative chemical change $\Delta T^+/T_0$, where ΔT^+ is due to changes in the refractive index of the membrane upon entrance of water during electroporation, are the quantities of choice.

Straightforward analysis shows that the vesicle/cell shape elongation parameter p can be related to the dichroism mode ΔT^-. For small elongation $p < 1.5$, where $p = c/b$ is the ellipsoidal axis ratio (c, the long axis; b, the short axis), ΔT^- is linearly proportional to $(p - 1)$. For very small elongations ($p \leq 1.13$), the relative increase in the membrane surface area $\Delta S/S_0$ at constant volume of the vesicle/cell interior is given by [9]

$$\frac{\Delta S}{S_0} \approx \frac{8}{45}(p - 1)^2 \quad (67)$$

Recalling Eq. (16) with $\Delta c = c^{\mathrm{in}} - c^{\mathrm{out}}$, the transmembrane difference in salt concentration and $\Delta c = 0$ for $c^{\mathrm{in}} = c^{\mathrm{out}}$, we readily see that:

$$\frac{(\Delta T^-)^{\Delta c}}{(\Delta T^-)^0} = \frac{p^{\Delta c}-1}{p^0-1} \approx \left(\frac{\Delta S^{\Delta c}}{\Delta S^0}\right)^{1/2} \tag{68}$$

Applying Eq. (5) yields the suggestive result:

$$\frac{f_p^{\Delta c}}{f_p^0} = \frac{K^{\Delta c}}{K^0} \approx \left(\frac{(\Delta T^-)^{\Delta c}}{(\Delta T^-)^0}\right)^2 \tag{69}$$

In this way, the turbidity mode ΔT^- provides a direct tool to determine, using Eq. (17), the difference in the Gibbs reaction energy terms

$$\Delta_r \hat{G}^{\Delta c} - \Delta_r \hat{G}^0 = -2RT\ell n\left[\frac{(\Delta T^-)^{\Delta c}}{(\Delta T^-)^0}\right] \tag{70}$$

2.6. Transport analysis

As already mentioned, the phenomenon of ME is coupled to secondary processes such as fusion of adjacent electroporated membranes (electrofusion) or to exchange of material from the inside to the outside [10,33] or from the outside to the inside [14,34,35]. The extent of material exchange may be operationally defined as a permeability ratio $r_{pm} = (\mathrm{Sig})/(\mathrm{Sig})_{\max}$, where a signal (Sig) is referred to its maximum value $(\mathrm{Sig})_{\max}$.

For electrohemolysis, $r_{pm} = \Delta\mathrm{OD}/\Delta\mathrm{OD}_{\max}$ is the fraction of hemolysed cells measured by the optical density (OD) of the released haemoglobin in the supernatant. The electroporative gene transfer defines $r_{pm} = T/T_{\max}$ as the ratio of maximally transformed cells [4,14]. Electroporative dye uptake is quantified by the ratio of coloured cells [34]. The ME secondary phenomena, covered by r_{pm}, oftenly only occur above a certain threshold value E_{th} of the electric field strength. Since ME is a continuous process without threshold features [2,11], the inequality $E \geq E_{th}$ refers to a critical range of $f_p \geq f_p^{\mathrm{crit}}$. The field strength where $r_{pm} = 1$ refers to $f_p(r_{pm} = 1)$ which may, or may not, be the maximum $f_p(\max)$ that is limited by the finite membrane conductivity caused by electropores. Indeed, many electropermeabilisation data suggest that $r_{pm} = 1$ is at a field strength far below $f_p(\max)$; see below. The experimental quantity r_{pm} may be expressed in terms of f_p, as graphically indicated in Fig. 1, according to:

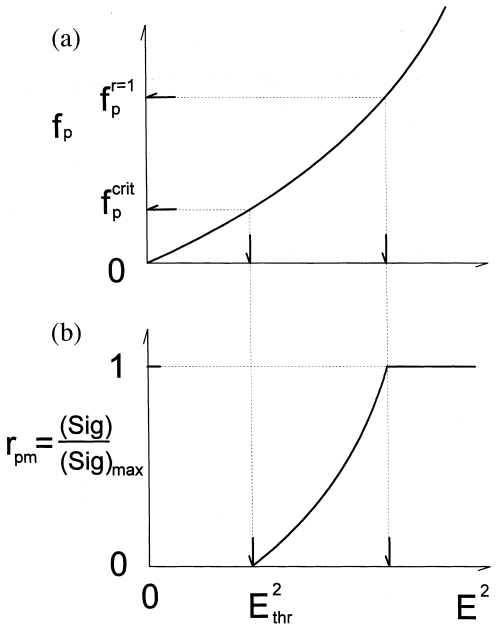

Fig. 1. Scheme for the relationship between pore fraction and permeability ratio: (a) f_p, (b) r_{pm} (electropermeabilization ratio), defined as the ratio of a measured signal to its maximum value, both as a function of E^2. Note, r_{pm} increases from a critical value $f_p = f_p^{\mathrm{crit}}$ at E_{thr} and levels off at $f_p = f_p^{r=1}$ (see Eqs. (71) and (72) of the text).

$$r_{pm} = \frac{f_p - f_p^{\mathrm{crit}}}{f_p(r_{pm}=1) - f_p^{\mathrm{crit}}} \tag{71}$$

The reason for the abscissa scaling in E^2 is Eqs. (10) and (20). Since always $K \approx f_p \leq 10^{-2}$ holds, f_p is proportional to $\exp[-b' \cdot E^2]$, where b' is a constant.

In the majority of previous studies, only the range $E \geq E_{thr}$, and thereby implicitly $f_p \geq f_p^{\mathrm{crit}}$, has been considered in using the practical approximation:

$$r_{pm} = f_p/f_p(r_{pm}=1) = b'' \cdot f_p \tag{72}$$

where b'' is a proportionality constant.

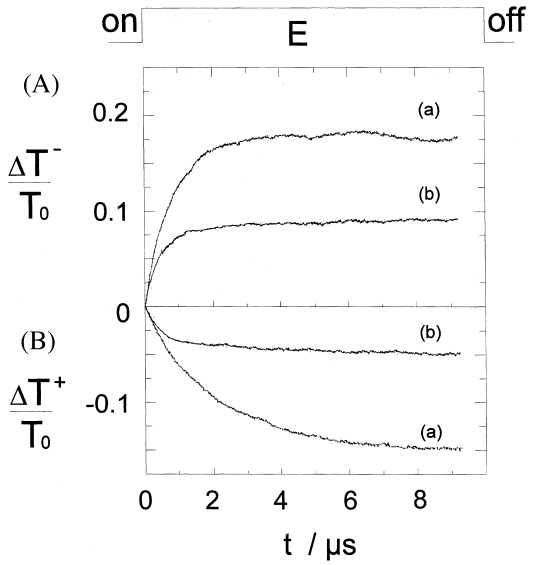

Fig. 2. Effect of electrolyte concentration on the time course of the field-induced relative turbidity changes ($\Delta T^{-}/T_0$) of lipid vesicles. (A) The dichroitic difference $\Delta T^{-}/T_0 = (\Delta T^{\parallel} - \Delta T^{\perp})/(T_0)$ and (B) the chemical sum $\Delta T^{+}/T_0 = (\Delta T^{\parallel} + 2\Delta T^{\perp})/(3T_0)$ of the relative turbidity changes at the parallel ($\Delta T^{\parallel}$) and perpendicular ($\Delta T^{\perp}$) light polarisation modes at $\lambda = 365$ nm: (a) at a large NaCl concentration difference: in the vesicle interior $c^{in} = [NaCl]^{in} = 0.2$ M, medium $c^{out} = [NaCl]^{out} = 0.2$ mM, osmotically balanced with 0.284 M sucrose and (b) at equal concentrations $c^{in} = c^{out} = 0.2$ mM. The unilamellar vesicles are composed of Avanti 20, total lipid concentration $[L_T] = 0.5$ mM; 0.66 mM HEPES (pH = 7.4), $T = 293$ K (20°C), vesicle radius $a_o = 160$ nm, vesicle density $\rho_V = 5.8 \times 10^{15}$ dm^{-1}. Application of one rectangular electric pulse, field strength $E = 4$ MV m^{-1} and pulse duration $t_E = 10$ μs [3].

3. Data analysis and discussion

3.1. Primary electrooptical relaxation data

The kinetic data in Fig. 2 demonstrate that both electrooptical turbidity relaxation modes, ΔT^{-} and ΔT^{+}, are larger for a finite transmembrane salt gradient $\Delta c = c^{in} - c^{out}$ as compared with $\Delta c = 0$. Obviously, in line with Eq. (19), ME is enhanced when the outside concentration of electrolyte of a vesicle (or cell) is small; note that here $\Delta c \approx c^{in} = 0.2$ M.

Fig. 3 shows that the salt gradient effect is dependent on the field strength, yet at higher field strengths the difference $f_p^{\Delta c} - f_p^0$ is roughly independent on E. The analysis of the ΔT^{-} and ΔT^{+} relaxations starts with the evaluation of the ellipsoidal elongation parameter p, reflecting the relative surface area increase. We use the numerical code method of Farafonov et al. [36], solving the electromagnetic scattering problem for confocal coated spheroids. The computer analysis, using the refractive index of the lipid membrane $n_\ell = 1.600$ (Avanti-20) and the medium $n_m = 1.3620$ of 0.284 M sucrose solution, $n_m = 1.3517$ for $c^{in} = c^{out} = 0.2$ mM and $n_m = 1.3517$ for $c^{in} = 0.2$ M, yields $p = 1.126$ at $c^{in} = c^{out} = 0.2$ mM and $p = 1.183$ at $c^{in} = 0.2$ M and $c^{out} = 0.2$ mM. The duration of the pulse $t_E = 10$ μs is too short for a measurable transport of electrolyte from the vesicle interior through the electropores to the bulk solution. Therefore the vesicle internal volume can be considered unchanged. The relative increase in the membrane surface area required to elongate a vesicle at constant volume is given by:

$$\Delta S/S_0 = p^{-2/3}/2 + p^{1/3} \cdot \arcsin\left(\sqrt{1-p^{-2}}\right) / \left(2 \cdot \sqrt{1-p^{-2}}\right) - 1 \quad (73)$$

For $p = 1.126$, we obtain $\Delta S/S_0 = 2.46 \cdot 10^{-3}$; for $p = 1.183$, $\Delta S/S_0 = 4.9 \cdot 10^{-3}$ (see also Neumann et al. [9]).

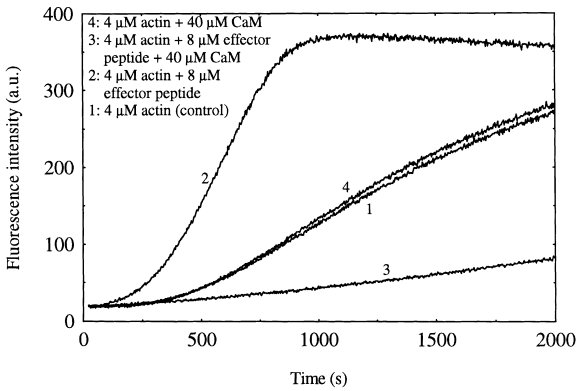

Fig. 3. Fraction $f_p = \Delta S_p/S_0 = N_p \cdot \langle r_p^2 \rangle / (4 \cdot a_o^2)$ of the electroporated membrane area of a vesicle/cell of surface $S_0 = 4 \cdot \pi \cdot a_o^2$, as a function of the external field strength E, calculated from the turbidity relaxations (in Fig. 2). ■, $f_p^{\Delta c}$, refers to $c^{in} = 10^3 \cdot c^{out} = 0.2$ M; ●, f_p^0, refers to $\Delta c = 0$, $f_p = f_p(0)$.

3.2. Characteristic electromechanical parameters

3.2.1. Stretching and undulation modes

In principle, the two main contributions to the electrically induced surface area increase $\Delta S = \Delta S_p + \Delta S_{ss}$ should be separable on the time scale. The contribution (ΔS_{ss}) due to stretching and smoothing of undulations should be more rapid than that of membrane electroporation (ΔS_p). The turbidity relaxation data in Fig. 2 do not permit to easily separate a rapid and a slow relaxation mode at $E = 4$ MV m^{-1}. Therefore we first estimate extent and time constant of a potential mode referring to ΔS_{ss}.

3.2.1.1. Amplitudes. Using a typical compression modulus of $K_s = 0.2$ Nm^{-1} and a bending rigidity $\kappa = 10^{-19}$ J [29] in the expression $\Delta S_{ss}/S_0 = kT \cdot \ell n\,(\xi/\xi_0)/(8\,\pi\kappa) + (\xi - \xi_0)/K_s$, where ξ and ξ_0 are the homogeneous lateral tensions in the presence and in the absence of an electric field, respectively [37], with $\xi \approx 3\ \varepsilon_0\ \varepsilon_w E^2/20$ [10]. Since $\kappa = K_s d^2/48 \approx 10^{-19}$ J [38], $\Delta S_{ss}/S_0 = \Omega/\kappa$, where $\Omega = kT \cdot \ell n\ (\xi/\xi_0)/(8\pi) + (\xi - \xi_0)d^2/48$. For $\Delta c = c^{in} - c^{out} = 0.2$ M, we obtain $\Delta\kappa = \Delta\kappa^{el} = -0.25 \times 10^{-19}$ J. The respective amplitude ratio for $\Delta c = 0.2$ M and $\Delta c = 0$ is given by $(\Delta S_{SS}^{\Delta c} - \Delta S_{SS}^{0})/\Delta S_{SS}^{0} = -\Delta\kappa^{el}/\kappa^{el} = 0.25$. On the other hand the actual amplitude ratio is $(4.9 - 2.46)/2.46 \approx 1$. Therefore, the data in Fig. 2 cannot only reflect the contribution of stretching and undulative smoothing. Rather, the major part must be due to ME. The extent of ME now is $f_p = (\Delta S - \Delta S_{ss})/S_0$. With $\Delta S_{ss}/S_0\ (c^{in} = 0.2$ mM$) = 1.6 \times 10^{-3}$ and $\Delta S_{ss}/S_0\ (c^{in} = 0.2$ M$) = 2.0 \times 10^{-3}$, the initial value of ξ_0 can be estimated: $\xi_0 \approx 3 \times 10^{-4}$ Nm^{-1}.

3.2.1.2. Time constant estimates. According to Komura (1996) the stretching time constant is given by $\tau_{str} \approx \eta a/K_s = 0.7$ ns [39], the undulation smoothing time constant $\tau_{und} \approx -(5\eta^3/16\kappa) \cdot \ln[1 - 64\,(p-1)\kappa/(3\varepsilon_0\varepsilon_w E^2 a^3)]$, where η is the viscosity. For $p = 1.126$, $\tau_{und} \approx 0.07$ μs; for $p = 1.183$, $\tau_{und} \approx 0.1$ μs. Both τ_{str} and τ_{und} are usually smaller than the interfacial polarisation time constant τ_{pol}, that is given by $\tau_{pol} = aC_m(\lambda_i^{-1} + \lambda_0^{-1}/2)$. With $C_m = 5 \times 10^{-3}$ F m^{-2}, $\lambda_i = 1.2$ S m^{-1} and $\lambda_0 = 2.6$ mS m^{-1} [see f_λ in the context of Eq. (25)], we obtain $\tau_{pol}\ (\Delta c = 0.2$ M$) = 0.47$ μs ($\lambda_i = 1.2$ S m^{-1}) and $\tau_{pol}\ (\Delta c = 0) = 0.16$ μs ($\lambda_i = \lambda_0 = 2.6$ mS m^{-1}).

Since the Maxwell–Wagner interfacial polarisation process is rate-limiting for the build-up of the transmembrane potential difference $\Delta\varphi_{ind}$, it also limits the kinetics of the stretching and undulation modes (≤ 0.5 μs). Because the actually observed time constants (see Fig. 2) $\tau\ (\Delta c = 0.2$ M$) = 0.6$ μs and $\tau\ (\Delta c = 0) = 0.9$ μs are larger than the τ_{pol}-values, the measured relaxations must be due to the slower process of electropore formation.

3.2.2. Electroporation parameters in salt gradients

3.2.2.1. Pore fractions. With $\Delta S_p = \Delta S - \Delta S_{ss}$ and Eq. (5) we obtain, $f_p^0 = 0.7 \times 10^{-3}$ at $c^{in} = c^{out} =$ 0.2 M NaCl and at $\Delta c \approx 0.2$ M NaCl, we have $f_p^{\Delta c} = 2.7 \times 10^{-3}$, yielding $f_p^{\Delta c}/f_p^0 = 3.9$. Using now Eq. (19), we see that $\Delta X = -[(\Delta_r\hat{G}^{\ominus})^{\Delta c} - (\Delta_r\hat{G}^{\ominus})^0] = 1.36\ RT$. On the other hand, the calculation of ΔX, using Eqs. (13), (18), (33), (40) and (52) or Eq. (65), and $\bar{r}_p = 0.35 \pm 0.05$ nm [6], $\sigma = 0.018$ Cm^{-2}, $N^{out} \approx N^{in}$, $\alpha \approx 1$ and $C_0 = C_0^{el}$, yields $\Delta X = 1.39\ RT$. This is close to the experimental value, suggesting that the theoretical results are consistent with the experimental data.

3.2.2.2. Salt gradient sensitivity. As seen in Fig. 4, the parameters C_0^{el}, κ^{el} and $\bar{\kappa}^{el}$ for vesicles change differently with increasing c^{in}, relative to a given $c^{out} = 0.2$ mM. The scaling parameter is the surface charge density. For instance, for $\sigma \leq 0.01$ Cm^{-2} the saturation levels at $c^{in} \approx 10^{-3}$ M clearly become visible, in line with the calculations of Winterhalter and Helfrich [25]. The opposite sign of C_0^{el} as a function of c^{in}, compared to κ^{el}, can be rationalised by the different nature of these parameters. Whereas C_0^{el} is only dependent on the differences in the s^2-terms [Eq. (59)], the parameters κ^{el} and $\bar{\kappa}^{el}$ are dependent on the absolute values of $s^2\ell$ and $\sigma s\ell^2$, see Eqs. (60) and (61), respectively.

For equal charge densities $\sigma = \sigma_{in} = \sigma_{out} = 0.01$ Cm^{-2} on both sides of the membrane and $c^{in} = c^{out} = 0.2$ mM, Eq. (62) yields: $C_0^{el} = -1.8 \times 10^7$

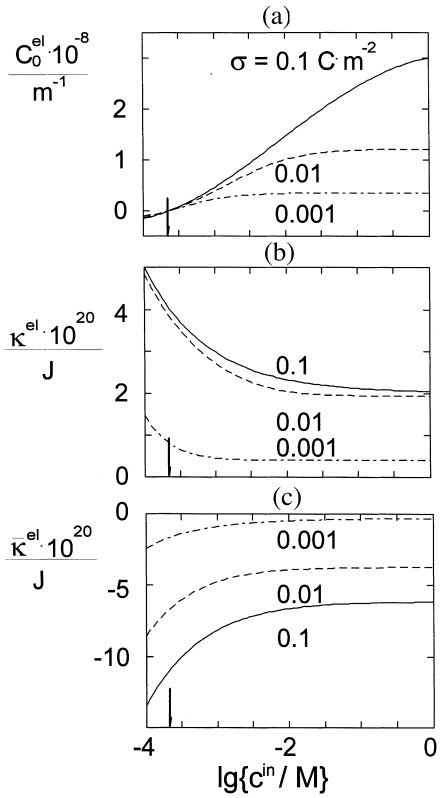

Fig. 4. Elasticity parameters of vesicle membranes. Electrostatic contributions C_0^{el} (a), κ^{el} (b) and $\bar{\kappa}^{el}$ (c) to the spontaneous curvature, bending rigidity and Gaussian elastic modulus, respectively, as a function of concentration c^{in} of NaCl in the vesicle interior. The calculations are performed here for the vesicle radius $a_o = 160$ nm, membrane thickness $d = 5$ nm, $T = 293$ K (20°C) and dielectric constant of water $\varepsilon_w = 80.4$ (293 K). The arrow indicates the electrolyte concentration equality $c^{in} = c^{out} = 0.2$ mM.

m^{-1}, $\kappa^{el} = 3.9 \times 10^{-20}$ J, $\bar{\kappa}^{el} = -7.0 \times 10^{-20}$ J. C_0^{el} is comparable to $1/a_0 = 0.63 \times 10^7$ m^{-1} for $a_0 = 160$ nm. If $C_0^{el} < 0$, it increases G_{bend}^{el}. If $c^{in} > c^{out}$, $C_0^{el} > 0$, contributing negatively to G_{bend}^{el} up to $C_0^{el} \leq 2/a_0$. For $C_0^{el} > 2/a_0$, C_0^{el} increases the bending energy. Generally, however, C_0^{el} may either increase or decrease G_{bend}^{el}.

It is further on remarked that the internal salt concentration c^{in} does not affect the outer membrane side. Therefore a change in c^{in}, here from $c^{in} = 0.2$ M to $c^{in} = 0.2$ mM, does not change $\Delta\varphi_{ind}$; $\Delta\varphi_{ind}$ may be, however, somewhat smaller than given by Eq. (25) [15]. The specific capacities of the two double layers C_{dlay}^{in} (0.2 M) $= \varepsilon_0\varepsilon_w/\ell_{in}$ $= 1.08$ F m^{-2} and C_{dlay}^{out} (0.2 mM) $= \varepsilon_0\varepsilon_w/\ell_{out} =$ 0.034 F m^{-2} are much larger than that of the membrane $C_m = 5 \times 10^{-3}$ F m^{-2}. Hence, they do not affect $\Delta\varphi_{ind}$ either. In addition, because of $f_p \ll 1$ ($f_p \approx 0.003$), the pore formation at lower field strength does not affect the conductivity

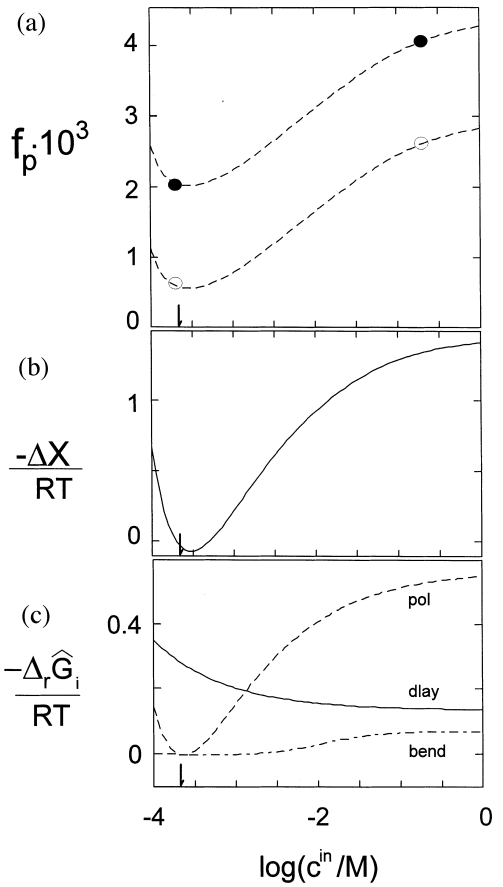

Fig. 5. Thermodynamic parameters of the vesicle membranes as a function of the logarithm of the NaCl concentration c^{in} in the vesicle interior at the constant outside concentration $c^{out} = 0.2$ mM: (a) the fraction f_p (dashed lines) of the electroporated membrane area; ○ and ●, f_p obtained from the analysis of the dichroitic turbidity mode $\Delta T^-/T_0$ and the chemical mode $\Delta T^+/T_0$ in Fig. 2 at $E = 4$ and 7 MV m^{-1}, respectively; (b) the difference $\Delta X = X^{\Delta c} - X^0$ of the ionic strength dependent standard Gibbs reaction energies $X^{\Delta c}$ (at $\Delta c > 0$) and X^0 (at $\Delta c = 0$) assuming cylindrical pores, $\bar{r}_p = 0.35 \pm 0.05$ nm; (c) individual contributions of $\Delta_r\hat{G}_{bend}$ (bend), $\Delta_r\hat{G}_{dlay}$ (dlay) and $\Delta_r\hat{G}_{pol}$ (pol), ($\kappa^{mech} = 10^{-19}$ J, $\sigma = 0.018$ C m^{-2}). The arrows ↓ refer to $c^{in} = c^{out}$ (see the text).

factor f_λ. Therefore, $f_\lambda = 1$ may be considered constant, independent of c^{in} in the range used here.

The presence of sucrose affects the dielectric constant ($\varepsilon_w = 80.4$ at 293 K) only slightly. At [sucrose] = 0.284 M, to balance the osmolarity of the 0.2 mM NaCl solution with 0.2 M NaCl, we obtain $\Delta\varepsilon = \varepsilon_w - \varepsilon(\text{suc}) = -1.2$ [40], thus $\varepsilon_w(\text{suc}) \approx \varepsilon_w$ is a good approximation.

As shown in Fig. 5, concomitant with f_p, it is the term $\Delta_r\hat{G}_{pol}$ in ΔX that controls the dependencies on c^{in}, showing a minimum near $c^{in} = c^{out}$. In the polarisation term, it is the contribution of $\Delta\varphi_s$ to $\Delta\varphi_m$ which renders it dominantly sensitive to salt gradients. The minimum in $-\Delta X/RT$ at $c^{in} \approx c^{out}$ visualises that, in line with experimental experience, membrane electroporation and thus electroporative permeability changes are facilitated only if there is a larger difference in the salt content between inside and outside of the vesicle or cell.

Fig. 6 clearly shows that it is again the dielectric polarisation term which, via the surface charge density, is most sensitive to salt concentration, in particular in the practical range between $0.005 \leq \sigma/\text{C m}^{-2} \leq 0.015$. Note that $\ell(0.2\text{ M}) = 0.7$ nm and $\ell(0.2\text{ mM}) = 20.8$ nm. Because $a_0 = 160$ nm, the approximation $\ell/a_0 \ll 1$ is applicable. On the same line, $(\varepsilon_w/\varepsilon_L)d = (80/2)\cdot 5\text{ nm} = 200$ nm, hence the approximation $\ell \ll (\varepsilon_w/\varepsilon_L)\cdot d$ holds throughout.

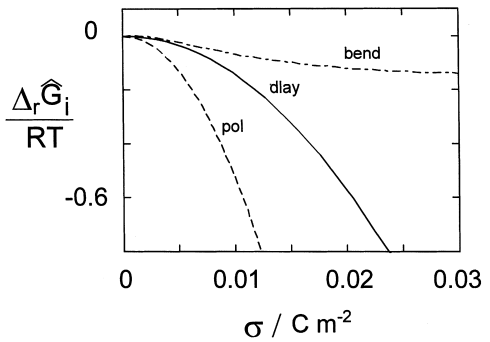

Fig. 6. The reaction Gibbs energies $\Delta_r\hat{G}_{bend}$ (bend), $\Delta_r\hat{G}_{dlay}$ (dlay) and $\Delta_r\hat{G}_{pol}$ (pol), all as a function of the surface charge density σ at $c^{in} = 0.2$ M and $c^{out} = 0.2$ mM, pore fraction $f_p^{\Delta c} = 0.003$; see also Fig. 5.

3.3. Electroporative permeability parameters

Fig. 7 shows that, using an already very simple approximation, Eq. (72), the permeability data can be well rationalised in terms of Eq. (71), displayed in Fig. 1. In Fig. 7, it is seen that r_{pm} increases with the transmembrane salt difference, expressed logarithmically as the difference $RT\cdot\ln(c^{in}/c^{out})$ of the chemical potentials at the salt concentrations. The concentrations c^{out} (with $c^{in} \approx 0.15$ M) have been estimated from the conductivity data. Apparently, at a given field strength, ME has already reached a membrane state where $r_{pm} = 1$, where the field effect causes maximum material exchange. Any further increase in the transmembrane gradient is ineffective.

In detail, the data show that r_{pm} increases with decreasing c^{out} (from λ_0) at constant c^{in}. Since a decrease in λ_0 decreases the factor f_λ in Eq. (25), a decrease in c^{out} should reduce the extent of ME and thus reduce r_{pm}. This is in contrast to the data (Fig. 7). Indeed, it is the increase in Δc and thus the increase in $\Delta X = -(\Delta_r\hat{G}^{\Delta c} - \Delta_r\hat{G}^0)$ which favours ME and thus increases r_{pm}. It appears that pore size and pore density must reach a certain threshold value before transport across the electroporated membrane can occur.

3.4. Entropic and adsorption contributions to C_0

Besides C_0^{el}, C_0 has been suggested to have two further contributions: a so called entropic term C_0^{entr} and an adsorption term C_0^{ad}. We may understand that addition of sucrose or salt to the solutions changes the solvent composition and thereby the interface between membrane and the adjacent solution. According to Lipowsky and Döbereiner [41] we have (in different notation):

$$C_0^{entr} = \frac{RT}{2\kappa}(r_i - r_{suc})(d + r_i + r_{suc})c^{in}x_{suc} \qquad (74)$$

where $r_i = r_{Na^+} \approx r_{Cl^-} \approx 0.15$ nm is the mean radius of the hydrated salt ions and $r_{suc} \approx 0.7$ nm that of the hydrated sucrose molecule; $x_{suc} = n_{suc}/(n_{suc} + 2\ n^{in})$ is the mole fraction of sucrose with $n^{in} = V\cdot c^{in}$, $c^{in} = 0.2$ mM referring to NaCl,

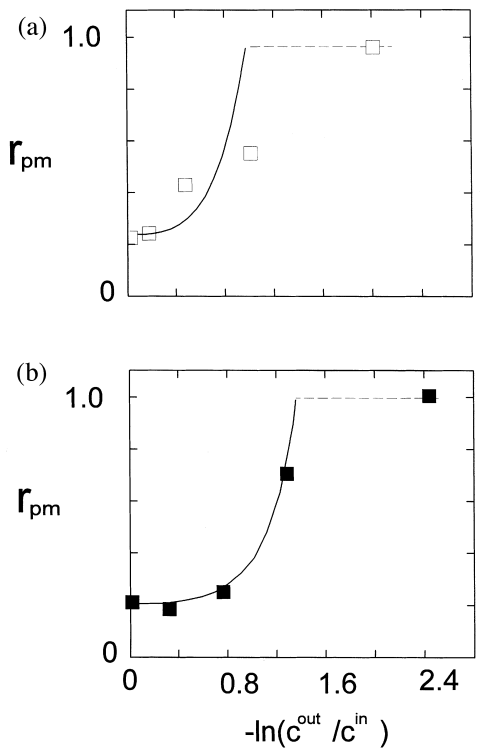

Fig. 7. Theoretical interpretation of electropermeabilization data: (a) haemolysis (H) data of human erythrocytes (r_{pm} = %H/100% H) of Sukhorukov et al. [47]; (b) field-induced uptake of the dye Trypan blue into human lymphoma cells U 937 (r_{pm} = blue-stained cells/total (blue-stained and unstained)) of Velizarov et al. [48], both as a function of the difference $\Delta c = c^{in} - c^{out}$. A typical value for the cell inside is $c^{in} \approx 0.15$ M. The outside concentrations c^{out} have been calculated from the conductivities given by the authors [47,48] The solid lines refer to the scaling approximation $r_{pm} = b \cdot f_p$ for $f_p^{crit} \le f_p \le f_p^{max}$, $E \ge E_{th}$ [see Eq. (72)].

i.e. Na^+-ions and Cl^--ions. Here $c_{suc} \approx 0.284$ M, hence $n_{suc} = 0.284\ M \cdot V$ and with $c^{in} = 0.2$ mM $x_{suc} \approx 1$. At $T = 293$ K and with $\kappa \approx 10^{-19}$ J and $\sigma = 0.018$ C m^{-2}, we estimate: $C_0^{entr} = -0.15 \times 10^8$ m^{-1}.

If the sucrose molecule is adjacent to the lipid head groups, it may be considered as adsorbed. The adsorption term is given by [41]:

$$C_0^{ad} = \frac{RT}{2\kappa}(d + 2r_{suc})\Gamma_{suc} \tag{75}$$

where Γ_{suc} is here the amount $n_{suc} = N_{suc}/N_A$ of N_{suc} molecules adsorbed per area unit. Using now $\Gamma_{suc} \approx \Gamma_{glu} = -1.4 \times 10^{-6}$ mol m^{-2} ($N_{suc} = 8.4 \times 10^{17}$ m^{-2}, the value of glucose near egg lecithin lipid membranes [42]), we estimate $C_0^{ads} = 1.1 \times 10^8$ m^{-1}[43].

It is realised that C_0^{entr} is smaller than C_0^{el}, but C_0^{ads} is similar to a the electrostatic contribution C_0^{el}. So far there is no reliable estimation for eventual differences between $(C_0^{entr})^P$ and $(C_0^{ads})^P$ in the pore state **P** compared to those C_0-values of the closed bilayer state **C**. Therefore, at present the Gibbs reaction energy terms $\Delta_r\hat{G}_{(entr)}$ and $\Delta_r\hat{G}_{(ads)}$, analogous to the other terms $\Delta_r\hat{G}_i$ contributing to the total $\Delta_r\hat{G}^{\ominus}$ have not been specified.

4. Conclusion

The theoretical analysis shows that transmembrane salt concentration gradients can significantly modify spontaneous curvature, bending rigidity and modulus of Gaussian curvature, if the electrostatic interactions between the charged groups of the lipids are affected. Different Debye screening lengths on the two membrane sides generate a difference in the surface potentials which in turn affects the extent of ME. Ionic strength-dependent alteration in the elastic parameters and the surface potentials may either facilitate or hinder the formation of electropores. Generally, large concentration gradients and high charge densities at the membrane water interface increase extent and rate of electric pore formation and the subsequent deformation of vesicles and cells in an electric field.

The experimental data of the turbidity dichroism of salt-filled vesicles are consistent with the theoretical approach. Therefore the theoretical framework developed in this study may provide guidelines for the optimisation of the experimental conditions for the electroporative transfer of drugs and genes to tissue cells.

Acknowledgements

We thank Frau M. Hofer for careful processing of the manuscript and the Deutsche Forschungs-

gemeinschaft (DFG) for the grant Ne 227/9-3 to E.N.

Appendix A: Gibbs equation for chemophysical processes

The fundamental Gibbs equation, generally applicable for isobaric–isothermal processes in a homogeneous phase α is given by [44]:

$$dG = -S'dT - Vdp + \Sigma_k x_k \cdot X_k \quad (A1)$$

where S' is entropy, V the volume, p the external pressure. The parameter x_k is the generalised force and X_k the generalised displacement of type k, respectively.

If p and T are same before and after the process, i.e. $dp = 0$ and $dT = 0$, the Gibbs energy function $G(x,X)_{p,T}$ relevant for ME reads:

$$dG = \Sigma_j \mu_j dn_j + EdM + \varphi dq + \Gamma dS + \gamma dL + \Sigma_k \beta_k dC_k \quad (A2)$$

For processes which can be controlled by externally applied electric fields it is appropriate to group together certain terms in Eq. (A2) according to:

$$dG = dG_{chem} + dG_{el} + \Sigma_i dG_i \quad (A3)$$

The chemical term dG_{chem}, referring to positional changes or to reactive changes of the molecules such as a conformational transitions, is given by:

$$dG_{chem} = \Sigma_j \mu_j dn_j \quad (A4)$$

and is discussed in the context of Eqs. (6) and (12) of the main text.

The electric term

$$dG_{el} = EdM \quad (A5)$$

covers the contribution of the external electric field E and the overall electric dipole moment M of a phase.

Other physical terms are presented in the sum $\Sigma_i dG_i$. For instance, surface or interfacial charges $q_s = \Sigma_j |z_j| \cdot e_0$, where z_j is the charge number (with sign) and e_0 the elementary charge, are accounted for by (i = surf):

$$dG_{surf} = \varphi_s dq_s \quad (A6)$$

where φ_s is the actual (eventually screened) electric surface potential at a point in the membrane/solution interface. The surface (or interface) tension Γ of the interface area S is represented by

$$dG_{tens} = \Gamma dS \quad (A7)$$

The interface of a lipid pore is associated with a higher Gibbs energy. This edge energy is given by:

$$dG_{line} = \gamma dL \quad (A8)$$

where γ is the line tension and L is the edge length; for a cylindrical pore $L = 2\pi \cdot \bar{r}_p$, where $\bar{r}_p = \sqrt{\langle r_p^2 \rangle}$ is the mean pore radius. The elastic curvature of a membrane may generally be covered by a bending term

$$dG_{bend} = \Sigma_k \beta_k dC_k \quad (A9)$$

where β_k is the generalised curvature force and C_k is the generalised curvature coordinate (reciprocal radius) of the type k, respectively. See Eq. (43) of the main text.

A.1. Geometrical curvature

In Eq. (A8), both the principal and the Gaussian curvatures as well as Helfrich's spontaneous (or chemical) curvature are covered. Classical differential geometry, see, e.g. Landau and Lifschitz (1991), provides an expression for the energy density of bending (g_{bend}) of a curved thin plate of the thickness d.

In Gibbs notation, the Gibbs energy required for a displacement dz relative to the X, Y-plane is given by:

$$G_{\text{bend}} = \oint \mathrm{d}S \cdot \frac{\kappa}{2} \cdot \left\{ \left(\frac{\partial^2 z}{\partial x^2} + \frac{\partial^2 z}{\partial y^2} \right)^2 + 2 \cdot (1 - \sigma_P) \cdot \left(\left(\frac{\partial^2 z}{\partial x \partial y} \right)^2 - \frac{\partial^2 z}{\partial x^2} \frac{\partial^2 z}{\partial y^2} \right) \right\} \quad \text{(A10)}$$

where $\oint \mathrm{d}S = S$ represents the surface considered. The energy parameter is specified by the elasticity or bending rigidity: $\kappa = E \cdot d^3/[12 \cdot (1 - \sigma_P^2)]$, where E is the elasticity (or tension) modulus, σ_P is the Poisson number characterising the transversal contraction of the plate, $\sigma_P = (3K - 2\mu)/[2(3K + \mu)]$, K (in Nm^{-2}) is the compression modulus, and μ (in Nm^{-2}) is the torsion modulus.

If the plate is a part of an ellipsoid of revolution with the symmetry axis Z, the displacement z is given by $z = c \cdot \sqrt{1 - (x^2 + y^2)/b^2}$, where b and c are the main semi-axes of the ellipsoid. Substitution of z in Eq. (A10) yields that $(\partial^2 z/\partial x \partial y)^2 - (\partial^2 z/\partial y^2) \cdot (\partial z/\partial y^2) = 0$, independent of the orientation of the symmetry axis of ellipsoid. The two principal curvatures of the ellipsoid can be expressed by $C_x = \partial^2 z/\partial x^2/(1 + (\partial z/\partial x)^2)^{3/2}$ and $C_y = \partial^2 z/\partial y^2/(1 + (\partial z/\partial y)^2)^{3/2}$. Around the zero point of the local coordinate system with Z-axis parallel to the membrane normal of a vesicle or a cell with c, $b \gg d$, the inequalities $(\partial z/\partial x)^2 \ll 1$ and $(\partial z/\partial y)^2 \ll 1$ are fulfilled, and the expressions for the principal curvatures C_x and C_y simplify to:

$$C_x = \partial^2 z/\partial x^2, \quad C_y = \partial^2 z/\partial y^2 \quad \text{(A11)}$$

Substitution into Eq. (A10) yields

$$G_{\text{bend}} = \oint \mathrm{d}S \cdot \left\{ \frac{\kappa}{2} \cdot (C_x + C_y)^2 \right\} \quad \text{(A12)}$$

covering the two principals curvatures $C_x = C_1$ and $C_y = C_2$ in Helfrich's notation.

A.2. Dipolo-(electro-) chemical potential

The adequate thermodynamic work potential for the description of electric field (E) effects is the characteristic [45] or the transformed [46] Gibbs energy, defined as:

$$\hat{G} = G - E \cdot M \quad \text{(A13)}$$

where the total moment is given by $M = \sum_j M_j \cdot n_j$, $M_j = N_A \langle m_j \rangle$, where M_j is the molar moment and $\langle m_j \rangle$ the orientational average of the electric dipole moment vector m_j of species j, respectively. In Guggenheim's notation, $M = V \cdot \varepsilon_0 \cdot \varepsilon \cdot E^2$ [45]

Applying Eq. (A3) in the reduced form for electric field effects,

$$\mathrm{d}G = \sum_j \mu_j \mathrm{d}n_j + E\mathrm{d}M \quad \text{(A14)}$$

and substituting in the differential form of Eq. (A13), we obtain

$$\mathrm{d}\hat{G} = \sum_j \mu_j \mathrm{d}n_j - M\mathrm{d}E \quad \text{(A15)}$$

where now E is the independent variable, as required. The differential operation $(\mathrm{d}\hat{G}/\mathrm{d}n_j)_{p,T,n \neq n_j} = \hat{\mu}_j = \mu_j - \int_0^E M_j \, \mathrm{d}E$ defines the dipolo-(or dielectro-) chemical potential [12], where the notation $n \neq n_j$ means all n constant except for n_j.

A.3. Chemophysical potential

The more general transformed Gibbs energy, adequate for the energetics of ME is an extension of Eq. (A15):

$$\mathrm{d}\hat{G} = \mathrm{d}G_{\text{chem}} + \mathrm{d}\hat{G}_{\text{pol}} + \sum_i \mathrm{d}G_i \quad \text{(A16)}$$

where the polarization Gibbs energy is defined by

$$\mathrm{d}\hat{G}_{\text{pol}} = -M\mathrm{d}E \quad \text{(A17)}$$

Applying Eq. (A3) and the differential operator $\mathrm{d}/\mathrm{d}n_j$ to Eq. (A16) we may formulate a generalised chemophysical potential according to

$$\hat{\mu}_j = \left(\frac{\partial \hat{G}}{\partial n_j}\right)_{p,T,n\neq n_j} = \mu_j + N_A \cdot \Sigma_k \int x_k \mathrm{d}X_k \quad \text{(A18)}$$

The standard value of the chemophysical potential specified for ME reads

$$\hat{\mu}_j^{\ominus} = \mu_j^{\ominus} - \int M_j \mathrm{d}n_j + N_A \cdot \Sigma_k \int x_k \mathrm{d}X_k \quad \text{(A19)}$$

and enters into $\hat{G}_m^{\alpha} = \Sigma_j (\nu_j \cdot \mu_j^{\ominus})_m^{\alpha}$ as discussed in the context of Eq. (6) of the main text.

A.4. Gibbs reaction energy terms

Applying the classical differential reaction operator $\Delta_r = d/\mathrm{d}\xi$, where $\mathrm{d}\xi = \mathrm{d}n_j/\nu_j$ is the differential molar advancement of the process (e.g. a state transition), n_j is the amount of substance and ν_j is the stoichiometric coefficient of component j, respectively, to Eq. (A16) we obtain the suggesting grouping:

$$\Delta_r \hat{G} = \Delta_r G_{\mathrm{chem}} + \Delta_r \hat{G}_{\mathrm{pol}} + \Sigma_{k'} \left(\Delta_r \hat{G}\right)_{k'} \quad \text{(A20)}$$

As outlined previously [2] the remaining physical terms k' can be specified according to Eq. (A2). For instance, Eq. (A7) yields $\Delta_r \hat{G}_{\mathrm{tens}} = N_A \cdot \int_0^S (\Gamma^P - \Gamma^C)\ \mathrm{d}S$; Eq. (A8): $\Delta_r \hat{G}_{\mathrm{line}} = N_A \cdot \int_0^L (\gamma^P - \gamma^C)\ \mathrm{d}L$ and Eq. (A9): $\Delta_r \hat{G}_{\mathrm{bend}} = N_A \cdot \int_0^C (\beta_i^P \cdot C_i^P - \beta_i^C \cdot C_i^C)\ \mathrm{d}C_i$.

Appendix B

The total electrostatic bending energy density $g_{\mathrm{bend}}^{\mathrm{el}}$ can be represented as the weighted sum between the inside (in) and outside (out) leaflets [25]:

$$g_{\mathrm{bend}}^{\mathrm{el}}(\mathrm{cyl}) = \frac{2}{a_{\mathrm{out}} + a_{\mathrm{in}}} \{a_{\mathrm{out}} \cdot g_{\mathrm{out}}^{\mathrm{el}}(\mathrm{cyl}) + a_{\mathrm{in}} \cdot g_{\mathrm{in}}^{\mathrm{el}}(\mathrm{cyl})\} \quad \text{(A21)}$$

$$g_{\mathrm{bend}}^{\mathrm{el}}(\mathrm{sph}) = \frac{2}{a_{\mathrm{out}}^2 + a_{\mathrm{in}}^2} \times \{a_{\mathrm{out}}^2 \cdot g_{\mathrm{out}}^{\mathrm{el}}(\mathrm{sph}) + a_{\mathrm{in}}^2 \cdot g_{\mathrm{in}}^{\mathrm{el}}(\mathrm{sph})\} \quad \text{(A22)}$$

The terms $g_{\mathrm{out}}^{\mathrm{el}}$ and $g_{\mathrm{in}}^{\mathrm{el}}$, each are developed as a power series of $1/a$, for a_{in} and a_{out}, respectively, according to:

$$g^{\mathrm{el}} = g_0 \pm (g_1 \cdot \ell) \frac{1}{a} + \left(g_1 \cdot \ell^2\right) \frac{1}{a^2} \quad \text{(A23)}$$

where the $-$ sign of the term $g_1 \cdot \ell$ refers to $g_1^{\mathrm{in}} \cdot \ell_{\mathrm{in}}$ and the $+$ sign to $g_1^{\mathrm{out}} \cdot \ell_{\mathrm{out}}$.

Substitution of Eq. (A23) into Eqs. (A21) and (A22) yields rather elaborate expressions. For instance, the cylinder term is:

$$g_{\mathrm{bend}}^{\mathrm{el}}(\mathrm{cyl}) = \frac{a_{\mathrm{in}}}{\bar{a}} \left\{ \left[g_0^{\mathrm{in}} + g_0^{\mathrm{out}} \cdot d' \right] - \left[\frac{g_1^{\mathrm{in}} \cdot \ell_{\mathrm{in}}}{a_{\mathrm{in}}} - \frac{g_1^{\mathrm{out}} \cdot \ell_{\mathrm{out}} \cdot d'}{a_{\mathrm{out}}} \right] + \left[\frac{g_2^{\mathrm{in}} \cdot \ell_{\mathrm{in}}^2}{a_{\mathrm{out}}^2} + \frac{g_{\mathrm{out}}^2 \cdot \ell_{\mathrm{out}}^2 \cdot d'}{a_{\mathrm{out}}^2} \right] \right\} \quad \text{(A24)}$$

where $d' = 1 + d/a_{\mathrm{in}}$. Comparison of the coefficients in Eqs. (55) and (56) of the text yields (a) for a cylinder shell:

$$\frac{\kappa^{\mathrm{el}} \cdot (C_0^{\mathrm{el}})^2}{\bar{a}} = \frac{a_{\mathrm{in}}}{\bar{a}} \cdot \{g_0^{\mathrm{in}}(\mathrm{cyl}) + g_0^{\mathrm{out}}(\mathrm{cyl}) \cdot d'\} \quad \text{(A25)}$$

$$-\frac{\kappa^{\mathrm{el}} \cdot C_0^{\mathrm{el}}}{\bar{a}} = -\frac{a_{\mathrm{in}}}{\bar{a}} \times \left\{ \frac{g_1^{\mathrm{in}}(\mathrm{cyl}) \cdot \ell_{\mathrm{in}}}{a_{\mathrm{in}}} - \frac{g_1^{\mathrm{out}}(\mathrm{cyl}) \cdot \ell_{\mathrm{out}} \cdot d'}{a_{\mathrm{out}}} \right\} \quad \text{(A26)}$$

$$\frac{1}{2} \cdot \frac{\kappa^{\mathrm{el}}}{\bar{a}^2} = \frac{a_{\mathrm{in}}}{\bar{a}} \times \left\{ \frac{g_2^{\mathrm{in}}(\mathrm{cyl}) \cdot \ell_{\mathrm{in}}}{a_{\mathrm{in}}^2} + \frac{g_2^{\mathrm{out}}(\mathrm{cyl}) \cdot \ell_{\mathrm{out}}}{a_{\mathrm{out}}^2} \cdot d' \right\} \quad \text{(A27)}$$

(b) for a spherical shell:

$$\frac{\kappa^{el}\cdot(C_0^{el})^2}{\bar{a}} = \frac{a_{in}}{\bar{a}}\{g_0^{in}(sph) + g_0^{out}(sph)\cdot d'\} \tag{A28}$$

$$-\frac{2\cdot\kappa^{el}\cdot C_0^{el}}{\bar{a}} = -\frac{a_{in}}{\bar{a}} \times\left\{\frac{g_1^{in}(sph)\cdot\ell_{in}}{a_{in}} - \frac{g_1^{out}(sph)\cdot\ell_{out}\cdot d'}{a_{out}}\right\} \tag{A29}$$

$$\frac{\bar{\kappa}^{el}+2\cdot\kappa^{el}}{\bar{a}^2} = \frac{a_{in}}{\bar{a}} \times\left\{\frac{g_2^{in}(sph)\cdot\ell_{in}}{a_{in}^2} + \frac{g_2^{out}(sph)\cdot\ell_{out}}{a_{out}^2}\cdot d'\right\} \tag{A30}$$

The coefficients g_0, g_1, g_2 have been obtained from the integral $g_{el} = \int_0^{\sigma}\varphi d\sigma$. The potential φ is the solution of the Poisson equation $\nabla^2\varphi = -\rho/(\varepsilon_0\cdot\varepsilon_w)$ in cylindrical or spherical coordinates, respectively, where ρ is the volume density of free ions and ∇ is the nabla operator. For a 1:1 electrolyte of concentration c, the Poisson–Boltzmann equation reads:

$$\nabla^2\varphi(R) = \frac{2\cdot c\cdot e_0}{\varepsilon_0\cdot\varepsilon_w\cdot N_A}\cdot\sinh\left(\frac{e_0\cdot\varphi(R)}{k\cdot T}\right) \tag{A31}$$

where $R = a/\ell$. Eq. (31) is now applied to each side (in/out) of the membrane. Note, for $\nabla^2\varphi$ in V m^{-2} computation may start with the conversion of c in mol m^{-3}. Assuming a uniform surface charge density σ [C m^{-2}] and charge neutrality for the bulk, the boundary conditions for φ are: (a) outside of the shell: $R = a/\ell \to \infty$ yields $\varphi(R) = 0$ and $d\varphi(R)/dR = 0$. At $R = a_{out}/\ell_{out}$, we have

$$-\frac{e_0}{kT}\cdot\frac{d\varphi(R)}{dR} = \frac{e_0\cdot\sigma_{out}\cdot\ell_{out}}{\varepsilon_0\cdot\varepsilon_w\cdot kT} \equiv s_{out} \tag{A32}$$

(b) inside: $R \to 0$ yields $|\varphi(R)| > 0$ and $|d\Psi(R)/dR| > 0$. At $R = a_{in}/\ell_{in}$, we have

$$\frac{e_0}{kT}\cdot\frac{d\varphi(r)}{dr} = \frac{e_0\cdot\sigma_{in}\cdot\ell_{in}}{\varepsilon_0\cdot\varepsilon_w\cdot kT} \equiv s_{in} \tag{A33}$$

The parameters s_{in} and s_{out} enter in Eq. (59) of the text. With $m(cyl) = 1$ and $m(sph) = 2$, the coefficients g_0, g_1, g_2 are generally expressed for both, the inside and the outside, respectively, as [25]:

$$g_0 = d''\cdot\left\{2\cdot\ln\left[\frac{s}{2} + \left(1+\frac{s^2}{4}\right)^{1/2}\right] - \frac{4}{s}\cdot\left[\left(1+\frac{s^2}{4}\right)^{1/2} - 1\right]\right\} \tag{A34}$$

$$g_1 = -\frac{4\cdot m\cdot d''}{s}\cdot\ln[x] \tag{A35}$$

$$g_2 = d''\cdot\left\{m^2\cdot\left[\frac{1}{s} + \frac{8}{s^3}\left(1+\frac{1}{(1+s^2/4)^{1/2}}\right)\right] - \frac{2\cdot m\cdot(m-1)}{s}\cdot D_1(\ln[x])\right\} \tag{A36}$$

where $d'' = \sigma\cdot kT/e_0$ and $x = (1 + (1 + s^2/4)^{1/2})/2$ and D_1 is the Debye function: $D_1(x) = \int_0^x (e^t - 1)^{-1}\cdot t\ dt$ of x, t being the dummy variable.

Whereas $g_0(cyl) = g_0(sph)$, we readily see that:

$$g_1(cyl) = -\frac{4\cdot d''}{s}\cdot\ln[x] \tag{A37}$$

$$g_2(cyl) = d''\cdot\left\{\frac{1}{s} + \frac{8}{s^3}\left(1+\frac{1}{(1+s^2/4)^{1/2}}\right)\right\} \tag{A38}$$

$$g_1(\text{sph}) = -\frac{8\cdot d''}{s}\cdot \ln[x] \tag{A39}$$

$$g_2(\text{sph}) = 4\cdot\left\{g_2(\text{cyl}) - \frac{d''}{s}\cdot D_1(\ln[x])\right\} \tag{A40}$$

As mentioned in the main text, the combination of Eqs. (A37), (A38), (A39) and (A40) with Eqs. (A25), (A26), (A27), (A28), (A29) and (A30) leads to Eqs. (57) and (58).

For a cylinder shell the electrical contribution to the modulus of Gaussian curvature $\bar{\kappa}^{el} = 0$. For the spherical shell $\bar{\kappa}^{el}$ is given by:

$$\bar{\kappa}^{el} = \frac{8\cdot\bar{a}^2}{a_{out}^2 + a_{in}^2} \times \frac{kT}{e_0}\cdot\left\{\frac{\sigma_{out}\cdot\ell_{out}^2}{s_{out}}\cdot D_1[y_{out}] + \frac{\sigma_{in}\cdot\ell_{in}^2}{s_{in}}\cdot D_1[y_{in}]\right\} \tag{A41}$$

where $y = \ln[(1+\beta)/2]$.

References

[1] E. Sackmann, Membrane bending energy concept of vesicle- and cell-shapes and shape transitions, The Seventh Datta Lecture, FEBS Lett. 346 (1994) 3–16.

[2] E. Neumann, S. Kakorin, K. Toensing, Fundamentals of electroporative delivery of drugs and genes, Bioelectrochem. Bioenerg. 48 (1999) 3–16.

[3] E. Neumann, E. Werner, A. Sprafke, K. Krüger, in: B.R. Jennings, S.P. Stoylov (Eds.), Electroporation Phenomena — Electro-Optics of Plasmid DNA and of Lipid Bilayer Vesicles (Colloid and Molecular Electro-Optics), IOP Publ. Ltd, Bristol, UK, 1992, pp. 197–206.

[4] E. Neumann, Membrane electroporation and direct gene transfer, Bioelectrochem. Bioenerg. 28 (1992) 247–267.

[5] E. Neumann, E. Boldt, in: M.J. Allen, S.F. Cleary, F.M. Hawkridge (Eds.), Membrane Electroporation: Biophysical and Biotechnical Aspects (Charge and Field Effects in Biosystems-2), Plenum Press, 1989, pp. 373–382.

[6] S. Kakorin, S.P. Stoylov, E. Neumann, Electro-optics of membrane electroporation in diphenylhexatriene-doped lipid bilayer vesicles, Biophys. Chem. 58 (1996a) 109–116.

[7] M. Eigen, L. DeMaeyer, in: S.L. Friess et al. (Ed.), Relaxation Methods (Techniques of Organic Chemistry, vol. 8(2)), Wiley, New York, 1963, pp. 495–1054.

[8] E. Neumann, S. Kakorin, Digression on membrane electroporation and electroporative delivery of drugs and genes, Radiol. Oncol. 32 (1998) 7–17.

[9] E. Neumann, S. Kakorin, K. Toensing, Membrane electroporation and electromechanical deformation of vesicle and cells, Faraday Discuss. 111 (1998) 111–125.

[10] S. Kakorin, E. Redeker, E. Neumann, Electroporative deformation of salt filled lipid vesicles, Eur. Biophys. J. 27 (1998) 43–53.

[11] E. Neumann, S. Kakorin, Electrooptics of membrane electroporation and vesicle shape deformation, Curr. Opin. Colloid Interface Sci. 1 (1996) 790–799.

[12] E. Neumann, Chemical electric field effects in biological macromolecules, Prog. Biophys. Mol. Biol. 47 (1986) 197–231.

[13] E. Neumann, in: E. Neumann, A.E. Sowers, C. Jordan (Eds.), The Relaxation Hysteresis of Membrane Electroporation (Electroporation and Electrofusion in Cell Biology), Plenum Press, New York, 1989, pp. 61–82.

[14] E. Neumann, S. Kakorin, I. Tsoneva, B. Nikolova, T. Tomov, Calcium-mediated DNA adsorption to yeast cells and kinetics of cell transformation, Biophys. J. 71 (1996) 868–877.

[15] C. Grosse, H.P. Schwan, Cellular membrane potentials induced by alternating fields, Biophys. J. 63 (1992) 1632–1642.

[16] H.N.W. Lekkerkerker, Contribution of the electrical double layer to the curvature elasticity of charged amphipilic monolayers, Physica A. 159 (1989) 319–328.

[17] W. Helfrich, Elastic properties of lipid bilayers: theory and possible experiments, Z. Naturforsch. 28c (1973) 693–703.

[18] L. Landau, E. Lifschitz, Elastitätstheorie, Bd. 7, Akademie Verlag, Berlin, 1991, p. 223.

[19] R.E. Waugh, Elastic energy of curvature-driven bump formation on red blood cell membrane, Biophys. J. 70 (1996) 1027–1035.

[20] H.-G. Döbereiner, E. Evans, M. Kraus, U. Seifert, M. Wortis, Mapping vesicle shapes into phase diagram: a comparison of experiment and theory, Phys. Rev. E 55 (1997) 4458–4474.

[21] W. Helfrich, Deformation of lipid bilayer spheres by electric fields, Z. Naturforsch. 29c (1974) 182–183.

[22] M. Winterhalter, W. Helfrich, Deformation of spherical vesicles by electric fields, J. Coll. Int. Sci. 122 (1988a) 583–586.

[23] M. Winterhalter, W. Helfrich, Effect of surface charge on the curvature elasticity of membranes, J. Phys. Chem. 92 (1988b) 6865–6867.

[24] D.J. Mitchell, B.W. Ninham, Curvature elasticity of charged membranes, Langmuir 5 (1989) 1121–1123.

[25] M. Winterhalter, W. Helfrich, Bending elasticity of electrically charged bilayers: coupled monolayers, neutral surfaces, and balancing stresses, J. Phys. Chem. 96 (1992) 327–330.

[26] A. Fogden, D.J. Mitchell, B.W. Ninham, Undulations of charged membranes, Langmuir 6 (1990) 159–162.

[27] S. Leikin, M.M. Kozlov, N.L. Fuller, R.P. Rand, Mea-

sured effects of diacylglycerol on structural and elastic properties of phospholipid membranes, Biophys. J. 71 (1996) 2623–2632.
[28] H. Aranda-Espinoza, A. Berman, N. Dan, P. Pincus, S. Safran, Interaction between inclusions embedded in membranes, Biophys. J. 71 (1996) 648–656.
[29] U. Seifert, R. Lipowsky, in: R. Lipowsky, E. Sackmann (Eds.), Morphology of Vesicles (Structure and Dynamics of Membranes 1A), Elsevier, North-Holland, 1995, pp. 403–463.
[30] U. Seifert, Configurations of fluid membranes and vesicles, Adv. Phys. 46 (1997) 13–137.
[31] K. Tönsing, S. Kakorin, E. Neumann, S. Liemann, R. Huber, Annexin V and vesicle membrane electroporation, Eur. Biophys. J. 26 (1997) 307–318.
[32] S. Kakorin, E. Neumann, Chemical electro-optics and linear dichroism of polyelectrolytes and colloids, Ber. Bunsenges. Phys. Chem. 100 (1996b) 721–722.
[33] E. Neumann, K. Rosenheck, Permeability changes induced by electric impulses in vesicular membranes, J. Membr. Biol. 10 (1972) 279–290, 14 (1973) 194–196.
[34] E. Neumann, K. Toensing, S. Kakorin, P. Budde, J. Frey, Mechanism of electroporative dye uptake by mouse B cells, Biophys. J. 74 (1998) 98–108.
[35] E. Neumann, M. Schaefer-Ridder, Y. Wang, P.H. Hofschneider, Gene transfer into mouse lyoma cells by electroporation in high electric fields, EMBO J. 1 (1982) 841–845.
[36] V.G. Farafonov, N.V. Voshinnikov, V.V. Somsikov, Light scattering by a core-mantle spheroidal particle, App. Optics 35 (1996) 5412–5426.
[37] M. Kummrow, W. Helfrich, Deformation of giant lipid vesicles by electric fields, Phys. Rev. A. 44 (1991) 8356–8360.
[38] R. Goetz, G. Gompper, R. Lipowsky, Mobility and elasticity of self-assembled membranes, Phys. Rev. Lett. 82 (1999) 221–224.
[39] S. Komura, in: M. Rosoff (Ed.), Shape Fluctuations of Vesicles (Vesicles), Marcel Dekker, Inc, New York, Basel, Hong Kong, 1996, pp. 197–236.
[40] J.B. Hasted, in: F. Franks (Ed.), Dielectric Properties (Water), Plenum Press, New York, 1973, pp. 405–458.
[41] R. Lipowsky, H.G. Döbereiner, Vesicles in contact with nanoparticles and colloids, Europhys. Lett. 43 (1998) 219–225.
[42] P.M. Bummer, G. Zografi, The association of D-glucose with unilamellar phospholipid vesicles, Biophys. Chem. 30 (1988) 173–183.
[43] H.G. Döbereiner, O. Selchow, R. Lipowsky, Spontaneous curvature of fluid vesicles induced by trans-bilayer sugar asymmetry, Eur. Biophys. J. 28 (1999) 174–178.
[44] J.W. Gibbs, Elementary Principals of Statistical Mechanics, Ox. Bow. Press, Woodbridge, Co, 1981, p. 44.
[45] E.A. Guggenheim, Thermodynamics, 5th ed., North Holland Publ. Co., Amsterdam, 1967, p. 35, 335.
[46] C.J.F. Böttcher, in: O.C. Van Belle, P. Bordewijk, A. Rip (Eds.), Theory of Electric Polarization, 6th rev, Elsevier, Amsterdam, 1973, p. 319.
[47] V. Sukhorukov, H. Mussauer, U. Zimmermann, The effect of electrical deformation forces on the electropermeabilization of erythrocyte membranes in low- and high-conductivity media, J. Membr. Biol. 163 (1998) 235–245.
[48] S. Velizarov, M. Reitz, B. Glück, H. Berg, Electropermeabilization and electrofusion of human cells modified by anaesthetic agents, Bioelectrochem. Bioenerg. 47 (1998) 89–96.